# Platelet-Activating Factor Acetylhydrolase Activity in Cerebrospinal Fluid of Children with Acute Systemic or Neurological Illness

Hyeun-Wook Chang, PhD,[1] Soonhak Kwon, MD,[2] Hengmi Kim, MD,[2] Kunsoo Lee, MD,[2] Misuk Kim, MP,[1] Taechul Moon, MP,[1] and Sukhwan Baek, PhD[3]

**Platelet-activating factor acetylhydrolase was analyzed in cerebrospinal fluid samples taken from children with a variety of neurological conditions (85 patients; mean age, 3.8 years) to determine it is involved in the defense mechanism against the toxic effect of inflammatory mediators in the central nervous system. A significant increase in cerebrospinal fluid activity was seen in the patients with meningitis and acute febrile illness in comparison with the control subjects. The activity was also significantly higher in the patients with meningitis than in the patients with inflammatory neurological diseases. In addition, the biochemical profile of cerebrospinal fluid platelet-activating factor acetylhydrolase was different from other known acetylhydrolases. These findings suggest that cerebrospinal fluid platelet-activating factor acetylhydrolase activity may be a sensitive marker of the host response to central nervous system infections.**

Ann Neurol 2002;51:760–763

Platelet-activating factor acetylhydrolase (PAF-AH) is the enzyme that hydrolyzes the inflammatory mediator platelet-activating factor (PAF) and phospholipids containing oxidized truncated fatty acids.[1] The enzyme is distributed widely in tissues and plasma and is thought to be a defense mechanism that protects the host against the toxic effects of PAF and other biologically active oxidized phospholipids. Higher levels of PAF-AH have been found in plasma and other body fluids in a variety of different diseases,[2–8] but few studies have been conducted to measure the level of PAF-AH in cerebrospinal fluid (CSF).[7] We, therefore, measured the PAF-AH level in CSF of children with a variety of conditions, including meningitis, to determine if it is involved in the central nervous system (CNS) defense mechanism against the injury.

From the [1]College of Pharmacy, Yeungnam University, Gyongsan, South Korea; [2]Department of Pediatrics, Kyungpook National University Hospital, Daegu, South Korea; and [3]College of Medicine, Yeungnam University, Daegu, South Korea.

Received Aug 27, 2001, and in revised form Jan 10, 2002. Accepted for publication Jan 16, 2002.

Address correspondence to Dr Kwon, Department of Pediatrics, Kyungpook National University Hospital, Samdeok 2-50, Joong-Gu, Daegu, 700-721, South Korea. E-mail: shkwon@knu.ac.kr

## Patients and Methods

We evaluated a total of 85 patients (55 boys and 30 girls), newborn to 14 years (mean age, 3.8 years) who had a spinal tap for a variety of reasons at the Department of Pediatrics, Kyungpook National University Hospital, Daegu, South Korea, between November 1999 and January 2001. PAF-AH activity was measured in CSF samples taken from children with a variety of different conditions during the acute phase. Patients studied included seven with meningitis, 12 with status epilepticus, four with CNS inflammatory diseases, 20 with acute systemic infections including bacteremia or urinary tract infections, 24 with acute leukemia/lymphoma receiving intrathecal chemotherapy, and 18 with other conditions (eg, Miller-Dieker syndrome and skin abscesses) as controls.

### *Measurement of the Platelet-Activating Factor Acetylhydrolase Activity*

For the measurement of the PAF-AH activity, the CSF samples (50μl) were incubated with 10pM (100,000cpm) of [$^3$H]-acetyl-PAF, 50mM Tris-hydrochloric acid (pH 7.4), and 5mM EDTA in a polypropylene microcentrifuge test tube at 37°C for 30 minutes. The reactions were stopped by the addition of 2.5ml of chloroform/methanol (4:1) and 250μl of distilled water. The reaction mixtures were then centrifuged at 3,000 rpm for about 10 minutes, and the supernatants (600μl) were used to measure the radioactivity to determine the amount of [$^3$H] acetate liberated. We defined one unit as the enzyme activity necessary to hydrolyze 1% of the substrate under the standard assay condition. The radioactivity was determined with a liquid scintillation counter.

### *Statistical Analysis*

The findings were reported as the mean plus or minus the standard deviation. The data were analyzed with a Kruskal-Wallis one-way analysis of variance on ranks and all pairwise multiple comparison procedures (Dunn's method) to determine the difference in median values of PAF-AH in CSF among the groups using the Sigmastat statistical analysis program (Jandel Scientific GmbH, Erkrath, Germany). The Mann-Whitney rank sum test and *t* test were used to compare the enzyme activity in CSF between the disease group and control group or between the two different conditions.

## Results

All subjects demonstrated the presence of PAF-AH in CSF, but levels of PAF-AH activity ranged from 1.8 to 68U (mean, 18.5U; SD, 13.2U). The activity of PAF-AH in the newborns (mean, 32.3U; SD, 13.0U) was higher than in the infants (mean, 20.4U; SD, 13.2U) or children (mean, 14.2U; SD, 10.4U; $p < 0.05$; Fig 1). There was no significant difference be-

 

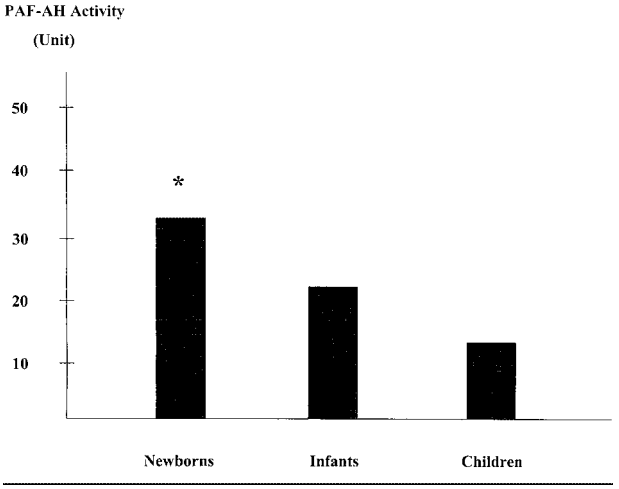


*Fig 1. Platelet-activating factor acetylhydrolase activity in cerebrospinal fluid by age. Platelet-activating factor acetylhydrolase activity in the newborns (mean, 32.3U; SD, 13.0U) is higher than in the infants (mean, 20.4U; SD, 13.2U) or children (mean, 14.2U; SD, 10.4U).* *$p < 0.05$.

tween the males (mean, 18.3U; SD, 11.2U) and females (mean, 19.0U; SD, 16.4U). PAF-AH activity was higher in the group with meningitis (mean, 39.3U; SD, 15.4U; $p < 0.01$) and in the group with acute systemic infection (mean, 30.6U; SD, 10.2U; $p < 0.01$) than in the control group, which had no acute illness (mean, 10.4; SD, 4.8U; Fig 2). However, there was no statistical difference between the acute systemic infection group and the group with meningitis ($p = 0.128$). The activity in the children on intrathecal chemotherapy for acute leukemia/lymphoma was low (mean, 11.2U; SD, 6.5U) and was not significantly different from that of the group with no acute illness (mean, 10.4U; SD, 4.8U). In the group with status epilepticus, PAF-AH activity was slightly higher (mean, 15.4U; SD, 9.7U) than that of the control group (mean, 10.4U; SD, 4.8U), but there was no significant difference between the two groups ($p = 0.227$). When we compared the meningitis group (mean, 39.3U; SD, 15.4U) to the group with inflammatory neurological diseases such as acute disseminated encephalomyelitis (mean, 18.6U; SD, 11.2U), there was a significant difference between the two groups ($p < 0.05$; see Fig 2).

## Discussion

The activity of PAF-AH has been measured in plasma and other body fluids in a variety of different diseases because it is thought to be involved in protecting cells against a variety of stresses. Bioactive PAF reportedly accumulates in the brain during injury, seizures, and ischemia.[9,10] However, few studies have been conducted to determine the cell types and mechanism responsible for the synthesis of PAF-AH or its role in the CNS.[11] The monocyte-macrophage system, endothelial cells, epithelial cells of the choroid plexus, or probably neuronal cells may be involved in this process, but further studies are needed for clarification. For this reason, we quantitatively and qualitatively analyzed PAF-AH in CSF of patients with a variety of different neurological conditions to see if it is involved in the CNS defense mechanism. Our study clearly demonstrates the presence of PAF-AH in CSF, but levels of PAF-AH activity ranged from 1.8 to 68U (mean, 18.5U; SD, 13.2U). The activity of PAF-AH in the newborns (mean, 32.3U; SD, 13.0U) was significantly higher than the activity in the infants (mean, 20.4U; SD, 13.2U) or children (mean, 14.2U; SD, 10.4U; $p < 0.05$; see Fig 1). Along with the results of an animal study, this finding suggests that human fetal and neonatal plasma PAF-AH activity may also be higher than the maternal values.[12] There was no significant difference between the males (mean, 18.3U; SD, 11.2U) and females (mean, 19.0U; SD, 16.4U). Because there were almost no data available on the normal values of PAF-AH in CSF, this study may provide a better understanding of CNS homeostasis. PAF-AH activity was higher in the group with meningitis (mean, 39.3U; SD, 15.4U; $p < 0.01$) and in the group with acute systemic infection (mean, 30.6U; SD, 10.2U; $p < 0.01$) than in the control group, which had no acute illness (mean, 10.4U; SD, 4.8U; see Fig 2). However, there was no statistical difference between the acute systemic infection group and the group with meningitis ($p = 0.128$). This finding indicates that the

*Fig 2. Platelet-activating factor acetylhydrolase activity in cerebrospinal fluid (CSF) under a variety of conditions. The activity in the meningitis group (mean, 39.3U; SD, 15.4U) and the acute systemic infection group (ASI; mean, 30.6U; SD, 10.2U) is higher than in the control group (mean, 10.4U; SD, 4.8U). There is a statistically significant difference between the meningitis group (mean, 39.3U; SD, 15.4U) and the inflammatory neurological disease group (IND; mean, 18.6U; SD, 11.2U).* *$p < 0.05$; **$p < 0.05$ *(a comparison between the meningitis and IND groups).*

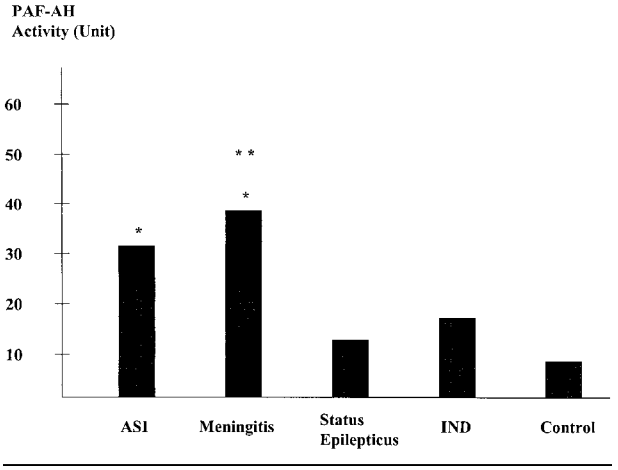

increase in CSF PAF-AH activity appears not to be due to overflow of the peripheral circulation into the intrathecal space, although the blood–brain barrier is damaged by meningitis. The activity in the children who were receiving intrathecal chemotherapy for acute leukemia/lymphoma was low (mean, 11.2U; SD, 6.5U), and there was no statistically significant difference from the control group (mean, 10.4; SD, 4.8U).

With respect to biochemical properties, PAF-AH in CSF was different from other known acetylhydrolases.[2–8,13–18] It is reported that plasma type PAF-AH has a higher molecular weight than the intracellular type and is resistant to protease.[13] We found that the enzyme PAF-AH in CSF hydrolyzed PAF as well as oxidized phosphatidylcholine at the *sn* −2 position. In addition, its molecular weight was estimated to be about 34KDa on 12.5% sodium dodecyl sulfate polyacrylamide gel electrophoresis (Fig 3). We also analyzed the effect of proteases and various chemical agents on the enzyme activity. The pH profile of the enzyme activity showed a broad optimum pH of 6.0 to 9.0. During purification, PAF-AH was different from phospholipase A2 in many aspects. The enzyme was not inhibited by idoacetamide, but it was inhibited by phenylmethylsulfonyfluoride and *p*-bromophenacybromide, suggesting that serine and histidine residues were required for the activity. In our study, PAF-AH activity in CSF showed a 1.5-fold increase with 0.1% chymotrypsin but remained unchanged with trypsin in the absence of 3-cholamidopropyl-dimethylammonio-1-propane-sulfate. Interestingly, when patients were treated with chymotrypsin and trypsin in the presence of 0.1% 3-cholamidopropyl-dimethylammonio-1-propane-sulfate, the enzyme activity increased about 2.5 and 1.5 times, respectively. On the basis of these results, the biochemical properties of PAF-AH in CSF were quite different from those of other known PAF-AH types. These findings suggest that PAF-AH in CSF might be a new PAF-AH isoenzyme.

*Fig 3. Biochemical profile of platelet-activating factor acetylhydrolase: lane M, molecular size marker; lanes 1 and 2, negative control; and lanes 3 to 5, platelet-activating factor acetylhydrolase from patients' cerebrospinal fluid. Platelet-activating factor acetylhydrolase bands are shown at 34KDa after electrophoresis on 12.5% polyacrylamide gels.*

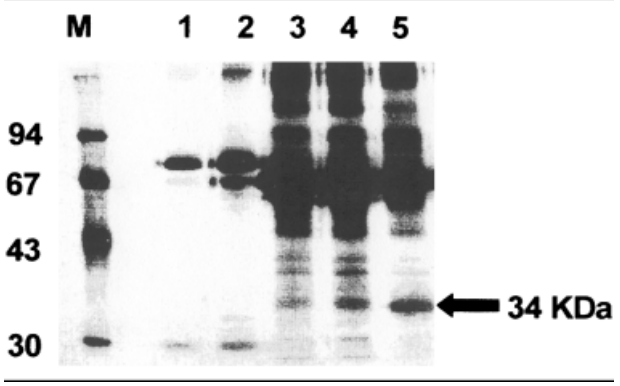


Cytosolic PAF-AH was reportedly markedly reduced after kainate-induced seizures in an animal study.[10] In our study, PAF-AH activity in CSF of the group with status epilepticus was slightly higher (mean, 15.4U; SD, 9.7U) than in the control group (mean, 10.4U; SD, 4.8U), but there was not a statistically significant difference between the two groups ($p = 0.227$). Surprisingly, when we compared the meningitis group (mean, 39.3U; SD, 15.4U) with an inflammatory neurological disease group, such as patients with acute disseminated encephalomyelitis (mean, 18.6U; SD, 11.2U), there was a significant difference between the two groups ($p < 0.05$; see Fig. 2). This suggests that PAF-AH may not play an important role in inflammatory neurological diseases, but further studies are needed. Recently, a few studies have indicated that intracellular PAF-AH activity may be involved in neuronal migration in the developing brain.[11,16,19,20] We had a patient with Miller-Dieker syndrome, and the enzyme activity was 7.6U, but it was not the lowest measured activity of all the patients.

In conclusion, we think PAF-AH may play an important role in protecting the host from a variety of CNS injuries. In addition, the PAF-AH activity in CSF may be a diagnostically useful marker of CNS infections such as meningitis. Recently, recombinant PAF-AH has become commercially available and is currently undergoing phase III trials for sepsis. We hope that it will be tested in the future as a therapeutic tool to protect the host from neuronal injuries such as meningitis.

## References


1. Min JH, Jain MK, Wilder Paul L, et al. Membrane-bound plasma platelet activating factor acetylhydrolase acts on substrate in the aqueous phase. Biochemistry 1999;38:12935–12942.
2. Morgan EN, Boyle EM Jr, Yun W, et al. Platelet-activating factor acetylhydrolase prevents myocardial ischemia-reperfusion injury. Circulation 1999;100:11365–11368.
3. Triggiani M, De Marino V, Sofia M, et al. Characterization of platelet-activating factor acetylhydrolase in human bronchoalveolar lavage. Am J Respir Crit Care Med 1997;156:94–100.
4. Narahara H, Tanaka Y, Kawano Y, et al. Platelet-activating factor acetylhydrolase activity in human follicular fluid. Adv Exp Med Biol 1996;416:121–127.
5. Ho YS, Swenson L, Derwenda U, et al. Brain acetylhydrolase that inactivates platelet-activating factor is a G-protein-like trimer. Nature 1997;385:89–93.
6. Tsuji H, Furukawa M, Ikeda H, et al. The presence of platelet-activating factor acetylhydrolase in human middle ear effusions. ORL J Otorhinolaryngol Relat Spec 1998;60:25–29.
7. Yutaka H, Shunro E, Tomoaki O, et al. Platelet-activating factor (PAF) concentration and PAF acetylhydrolase activity in cerebrospinal fluid of patients with subarachnoid hemorrhage. J Neurosurg 1994;80:31–36.

8. Hattori K, Adachi H, Tsujimoto, Arai H, Inoue K. Purification and characterization of platelet-activating factor acetylhydrolase II from bovine liver cytosol. J Biol Chem 1995;271: 33032–33038.
9. Kumar R, Harvey SA, Kester M, et al. Production and effects of platelet-activating factor in the rat brain. Biochim Biophys Acta 1988;963:375–383.
10. Shmueli O, Cahana A, Reiner O. Platelet-activating factor (PAF) acetylhydrolase activity, LIS1 expression and seizures. J Neurosci Res 1999;57:176–184.
11. Manya H, Aoki J, Watanabe M, et al. Switching of platelet-activating factor acetylhydrolase catalytic subunits in developing rat brain. J Biol Chem 1998;273:18567–18572.
12. Contador M, Moya FR, Zhao B, et al. Effects of dexamethasone on rat plasma platelet activating factor acetylhydrolase during the perinatal period. Early Hum Dev 1997;47:167–176.
13. Blank ML, Hall MN, Grees EA, Snyder F. Inactivation of 1-alkyl-2-acetyl-sn-glycero-3-phosphocholine by a plasma acetylhydrolase; higher activities in hypertensive rats. Biochem Biophys Res 1983;113:666–671.
14. Stafforini DM, Prescott SM, McIntyre TM. Human plasma platelet-activating factor acetylhydrolase: association with lipoprotein particles and role in the degradation of platelet-activating factor. J Biol Chem 1987;262:4223–4230.
15. Karasawa K, Yato M, Setaka M, Nojima S. Purification and characterization of platelet-activating factor acetylhydrolase from peritoneal fluid obtained from guinea pigs after endotoxin shock. J Biochem 1994;116:374–379.
16. Matsuzawa A, Hattori K, Aoki J, et al. Protection against oxidative stress-induced cell death by intracellular platelet-activating factor acetylhydrolase II. J Biol Chem 1997;272: 32315–32320.
17. Sapir T, Elbaum M, Reiner O. Reduction of microtubule catastrophe events by LIS1, platelet-activating factor acetylhydrolase subunit. EMBO J 1997;16:6977–69784.
18. Karasawa K, Kato H, Setaka M, Nojima S. Accumulation of platelet-activating factor acetylhydrolase in peritoneal cavity of guinea pig after endotoxin shock. J Biochem 1994;116: 368–373.
19. Adachi T, Aoki J, Manya H, et al. PAF analogues capable of inhibiting PAF acetylhydrolase activity suppress migration of isolated cerebellar granule cells. Neurosci Lett 1997;235: 133–136.
20. Albrecht U, Abu-Issa R, Ratz B, et al. Platelet-activating factor acetylhydrolase expression an activity suggest a link between neuronal migration and platelet-activating factor. Dev Biol 1996;180:579–593.

# Activity of the Hypothalamic–Pituitary–Adrenal Axis in Multiple Sclerosis: Correlations with Gadolinium-Enhancing Lesions and Ventricular Volume

Erina M. Schumann, MD, Tania Kümpfel, MD, Florian Then Bergh, MD, Claudia Trenkwalder, MD, Florian Holsboer, MD, PhD, and Dorothee P. Auer, MD

**The known interaction between the immune system and the hypothalamic–pituitary–adrenal axis led us to explore the interrelation between magnetic resonance imaging findings and the hypothalamic–pituitary–adrenal axis activity in 53 multiple sclerosis patients. The cortisol release induced by the dexamethasone-corticotropin-releasing hormone test was negatively associated with the presence and number of gadolinium-enhancing lesions and positively associated with ventricular size. This finding suggests a protective effect of the hypothalamic–pituitary–adrenal drive on acute lesional inflammation in multiple sclerosis, probably by limiting immune overshoot. In contrast, the nature of the correlation between hypothalamic–pituitary–adrenal hyperdrive and brain atrophy remains to be determined.**

Ann Neurol 2002;51:763–767

In multiple sclerosis (MS), autoimmune-mediated response is thought to be pathogenically relevant. As communication between the immune and neuroendo-

From the Max Planck Institute of Psychiatry, Munich, Germany.

Received Feb 22, 2001, and in revised form Jan 10, 2002. Accepted for publication Jan 19, 2002.

Published online May 3, 2002, in Wiley InterScience (www.interscience.wiley.com). DOI: 10.1002/ana.10187

Current address for Dr Schumann: Friedberg Hospital, Friedberg, Germany.

Current address for Dr Kümpfel: Department of Neurology, Ludwig-Maximilians-Universität München, Munich, Germany.

Current address for Dr Then Bergh: Laboratory of Molecular Biology, National Institute of Neurological Disease and Stroke, Bethesda, MD.

Current address for Dr Trenkwalder: Department of Clinical Neurophysiology, University of Göttingen, Göttingen, Germany.

Address correspondence to Dr Auer, Max Planck Institute of Psychiatry, Kraepelinstrasse 10, 80804 Munich, Germany.
E-mail: auer@mpipsykl.mpg.de

 

crine systems is bidirectional,[1] neuroendocrine dysfunction may well contribute to the pathogenesis and course of MS. This interaction has been investigated in preclinical and clinical studies, with an emphasis on the hypothalamic–pituitary–adrenal (HPA) axis, which is of central importance to the regulation of the immune system.[1] Observations in experimental allergic encephalomyelitis (EAE) have indicated that differences in inflammatory response may be induced by neuroendocrine–immune interactions. The main effect in EAE was attributed to the ability of the HPA axis to release sufficient levels of corticosteroids for the suppression of immune responses.[2–4]

To evaluate whether a similar interplay exists in MS patients, we compared surrogate markers of disease activity and atrophic changes, as derived from magnetic resonance imaging, with the results of the most sensitive test of the HPA axis function, the combined dexamethasone-suppression/corticotropin-releasing hormone stimulation (Dex-CRH) test.[5] We hypothesized that gadolinium (Gd)-enhancing lesions reflecting acute inflammatory disease activity[6] would be low in HPA hyperresponding patients. In addition, potential associations between brain atrophy measured by the normalized ventricular volume (VVn) and the activity of the HPA system were analyzed.

## Patients and Methods

### *Patients*

A total of 53 patients with clinically definite MS according to the Poser criteria (ie, 35 relapsing–remitting, 13 secondary progressive, and 5 primary progressive; Table 1) were included in this study. None of the patients had ever been treated with any immunomodulating agents, with the exception of intermittent, short-term, and high-dose glucocorticoids for relapses in 30 patients. Patients had to be free from glucocorticoid therapy for at least 6 weeks before admission so that intervening effects on Gd-enhancing lesions[7] and the Dex-CRH test results were excluded.[8] The study was approved by the local ethics committee, and written informed consent was obtained from each subject.

### *Dexamethasone-Suppression/Corticotropin-Releasing Hormone Stimulation Test Procedure*

The combined Dex-CRH test was performed according to a standardized protocol described previously.[5] The day before the corticotropin-releasing hormone stimulation (CRH) challenge, 1.5mg of dexamethasone was given orally. The following day, plasma cortisol levels were measured every 15 minutes from 15:00 to 16:30 hours, the first time point representing baseline postdexamethasone cortisol concentrations ($Bas_{Cort}$), and the remainder occurred after the CRH challenge at 15:02 (Clinalfa, Läufelingen, Switzerland). The maximum rise of cortisol after CRH injection with respect to $Bas_{Cort}$ ($\Delta_{max_{Cort}}$) and the area under the concentration–time curve of cortisol ($AUC_{Cort}$) were calculated. The patients were subdivided into a group with low $AUC_{Cort}$ values (hyporesponders) and a group with high $AUC_{Cort}$ values (hyperresponders) by the exclusion of patients whose cortisol levels were within the normal range, defined as the mean plus or minus the standard error of the mean of $AUC_{Cort}$ (mean, 150.76ng/ml; SEM, 34.14ng/ml) of 29 age-matched (mean, 32.8 years; SD, 9.0 years; men, 18; women, 11), healthy subjects from the institutional database.

### *Magnetic Resonance Imaging*

Brain magnetic resonance imaging was performed on a 1.5T magnetic resonance imaging unit (Signa Echospeed, General Electric Medical Systems, Milwaukee, WI). Precontrast and postcontrast (Gd-chelate [Omniscan] at a dose of 0.1mmol/kg) T1-weighted images (TR/TE, 640/14msec; slice thickness, 4mm) of 45 of the 53 MS patients were available for analyzing the presence ($Gd^+$ or $Gd^-$) and number of Gd-enhancing lesions ($nGd^+$). T2-weighted images (TR/TE, 3,600/70msec; slice thickness, 4mm) were used to estimate the volume of all ventricles and the total intracranial volume with Stobis software (courtesy of N. Roberts), which applies the Cavalieri principle of stereology.[9] The ventricular volumes were normalized (VVn) to the patient's individual intracranial volume.

### *Statistics*

Multivariate analyses of variance, followed by univariate *F* tests, were used to compare different groups. Age, duration of disease, and number of previous steroid therapies were

*Table 1. Clinical Characteristics of Multiple Sclerosis Patients*

| Group | n | Sex F/M | Age (yr) | Disease Duration (yr) | Relapse n | EDSS score (range) | No. of Previous Steroid Therapies |
|---|---|---|---|---|---|---|---|
| RR MS | 35 | 23/12 | 33.3 ± 8.3 | 3.6 ± 4.1 | 23 | 2.4 ± 1.0 (1–4) | 0.8 ± 1.2 |
| SP MS | 13 | 9/4 | 41.9 ± 8.8 | 15.7 ± 7.5 | 5 | 4.6 ± 1.6 (2.5–7.0) | 1.3 ± 1.2 |
| PP MS | 5 | 3/2 | 54.4 ± 7.2 | 5.1 ± 4.5 | 0 | 4.0 ± 1.0 (3.0–5.5) | 0.4 ± 0.5 |

Values are mean ±SD.

MS = multiple sclerosis; RR = relapsing–remitting; SP = secondary progressive; PP = primary progressive; EDSS = Kurtzke's Expanded Disability Status Scale.

used as covariates. For correlation analysis, we used Spearman's ρ test. For the reduction of type I error, all tests were followed by Bonferroni's post hoc correction for multiple tests.

## Results

The cortisol response of MS patients with Gd-enhancing lesions was different from that of patients without Gd-enhancing lesions ($F = 4.170$, $p = 0.011$; Table 2). This was attributable to lower $Bas_{Cort}$ and $AUC_{Cort}$ values in the $Gd^+$ group ($F = 11.016$, $p = 0.002$, and $F = 7.862$, $p = 0.008$, respectively). The covariates (age, duration of disease, and number of previous steroid therapies) had no significant effect. Moreover, there was an inverse correlation between $nGd^+$ and $AUC_{Cort}$ ($r = -0.442$, $p = 0.002$). In contrast, VVn correlated positively with $AUC_{Cort}$ ($r = 0.446$, $p = 0.001$), and this association remained after correction for the duration of the disease effect (partial correlation $r = 0.354$, $p = 0.012$).

Moreover, cortisol response in the Dex-CRH test had a clear effect on morphological characteristics, as shown by a comparison between hyporesponders and hyperresponders ($F = 8.855$, $p = 0.001$). Hyporesponders showed more $Gd^+$ lesions ($F = 7.040$, $p = 0.013$) and a lower VVn ($F = 6.248$, $p = 0.019$) than hyperresponders (Table 3).

As expected, the duration of disease had a significant covariate effect on VVn, whereas age or previous steroid therapies exerted no effect. To exclude potential confounds from the heterogeneity of the patient group, we repeated the comparison for the relapsing–remitting MS subgroup alone, which displayed similar differences ($F = 5.037$, $p = 0.02$).

## Discussion

The inverse correlation between $AUC_{Cort}$ in the Dex-CRH test and $nGd^+$ in our study provides the first clinical evidence that the HPA axis may have a modulatory effect on inflammatory disease activity in MS: high HPA activity appears to be protective, whereas low activity may promote blood–brain barrier breakdown. This finding is well in line with the known role of the HPA response in preventing immune overshoot[1] and observations in animal models of MS. The capacity of the HPA axis to induce endogenous corticosteroids that then inhibit cytokine production[1] is an important factor in limiting disease activity. A stress-induced increase in HPA axis activity or treatment

*Table 2. Hormone Data of Controls and Multiple Sclerosis Patients*

| Hormone Data | Control Group (n = 29) | MS Group (n = 53) | $Gd^+$ group (n = 28) | $Gd^-$ group (n = 17) |
|---|---|---|---|---|
| $Bas_{Cort}$ ng/ml | 8.0 ± 4.7 | 28.4 ± 27.4 | 18.4 ± 16.3 | 42.3 ± 32.1[b] |
| $\Delta_{max_{Cort}}$ ng/ml | 31.9 ± 45.1 | 40.3 ± 51.4 | 32.3 ± 43.8 | 52.5 ± 60.1 |
| $AUC_{Cort[AU]}$ | 150.8 ± 183.9 | 302.3 ± 255.9[a] | 217.0 ± 211.3 | 428.6 ± 294.4[b] |

Values are mean ±SD.

[a] $p < 0.05$ compared with controls.
[b] $p < 0.05$ compared with $Gd^+$ group.

MS = multiple sclerosis; $Gd^+$ group = MS patients with gadolinium-enhancing lesions; $Gd^-$ group = MS patients without gadolinium-enhancing lesions; $Bas_{Cort}$ = baseline concentration of cortisol after dexamethasone pretreatment before CRH challenge; $\Delta_{max_{Cort}}$ = maximum rise of cortisol after hCRH injection minus $Bas_{Cort}$; $AUC_{Cort}$ = area-under-the-concentration time curve of cortisol, AU = arbitrary units.

*Table 3. Hormone and Magnetic Resonance Imaging Data of Multiple Sclerosis Patients with Subnormal (Hyporesponders) and Exaggerated (Hyperresponders) Cortisol Response in the Dex-CRH Test*

| | Hyporesponders, All MS Patients (n = 13) | Hyperresponders, All MS Patients (n = 29) | Hyporesponders, RR MS n = 11 | Hyperresponders, RR MS n = 16 |
|---|---|---|---|---|
| $AUC_{Cort}$ [AU] | 69.2 ± 25.0 | 465.1 ± 243.5 | 72.0 ± 26.4 | 370.0 ± 159.8 |
| $nGd^+$ | 3.8 ± 1.3[a] | 1.0 ± 1.5 | 4.0 ± 5.0[b] | 1.1 ± 1.8 |
| | n = 12 | n = 22 | n = 10 | n = 11 |
| VVn (%) | 1.8 ± 1.0[a] | 2.8 ± 1.2 | 1.5 ± 0.5 | 2.4 ± 1.0 |
| | n = 12 | n = 28 | n = 10 | n = 16 |

Values are mean ±SD.

[a] $p < 0.05$ compared with hyperresponders of the total MS group.
[b] $p < 0.05$ compared with hyperresponders of the RR MS group.

Dex-CRH = dexamethasone suppression/corticotropin-releasing hormone (stimulation test); MS = multiple sclerosis; RR = relapsing-remitting; $AUC_{Cort}$ = area-under-the-concentration time curve of cortisol; AU = arbitrary units; $nGd^+$ = number of Gd-enhancing lesions; VVn = normalized ventricular volume.

with exogenous corticosteroids was found to downregulate the immune response in EAE, whereas a genetic deficiency in endogenous glucocorticoids, adrenalectomy, or treatment with the steroid receptor antagonist RU486 induces clinical exacerbation of EAE and increases the severity of inflammatory responses.[2–4,10] In contrast, no association was established between HPA axis characteristics and the susceptibility of developing EAE,[11] suggesting that individual variability in the HPA axis activity in MS patients can modulate the course of the disease rather than change the risk for acquiring the disease. The therapeutic effect of high-dose glucocorticoid treatment has been well established for optic neuritis, acute relapses in relapsing–remitting disease with a transient reduction of $nGd^{+}$.[7] Moreover, pulsed intravenous methylprednisolone therapy was recently shown to improve clinical outcome and to delay the progression of MR surrogate markers in relapsing–remitting MS.[12]

Our findings are also in good agreement with a study in which the net increase in $AUC_{Cort}$ in the CRH test was found to be negatively correlated with plasma log C-reactive protein,[13] which in turn has been shown to be raised during magnetic resonance imaging activity.[14] In contrast, Fassbender and coworkers[15] observed an opposite effect in 23 patients with relapsing–remitting MS (ie, patients with Gd-enhancing lesions showed an HPA hyperdrive). The discrepancy is difficult to explain, resulting most likely from clinical specificities of their sample including only patients with an acute relapse with a remarkably low rate of Gd enhancement of either brain or cord (only 8 of 23).

The positive correlation between $AUC_{Cort}$ and the ventricular volume supports the notion that HPA axis activity may increase with disease progression.[16] Moreover, we could show that this association was not simply an effect of the duration of the disease. Therefore, a direct interrelation between HPA hyperactivity and neurodegeneration in MS appears likely, but the direction of the effect remains obscure. Axonal damage in MS has been shown to occur even at an early stage of the disease,[17] so one might speculate that disease-related damage of neuronal networks involved in HPA system regulation may account for an altered cortisol response. However, this would not be in line with the observations that HPA axis dysregulation is modifiable by pharmacological intervention[8] and has also been reported during chronic inflammatory stress in animals insensitive to encephalopathy.[18] In contrast, elevated cortisol may enhance neurodegenerative processes in MS similarly to the suggested pathogenesis of hippocampal atrophy in major depressive disorder.[19] Because HPA axis hyperactivity appears to be more pronounced in secondary progressive MS compared with relapsing–remitting MS[16] and most hyporesponders in our study were found among relapsing–remitting MS patients, a gradual change in HPA axis function may occur over the course of MS. There is substantial evidence that HPA hyperdrive may reflect a functional disturbance of corticosteroid receptor-mediated negative feedback with a gradual increase in the arginine vasopressin/CRH ratio in the hypothalamic paraventricular nucleus,[20] probably to maintain HPA axis responsivity during glucocorticoid elevation in chronic inflammatory disease.

It is noteworthy that some MS patients showed a hyporesponding HPA axis despite high inflammatory stress, with cytokines such as interleukin-1, interleukin-2, and interleukin-6, tumor necrosis factor-$\alpha$, and interferon-$\gamma$, all potent activators of the HPA system.[1] Heterogeneity of the HPA function may, therefore, contribute to the large interindividual differences in disease activity in MS patients.[21] There is accumulating evidence that inflammatory disease activity is correlated with cerebral atrophy and clinical worsening in longer term studies.[22,23] Therefore, an investigation of the HPA axis early in the disease process may provide a new tool with which to assess the vulnerability to extensive disease activity and may modify individual therapeutic strategies.

We thank Rosa Hemauer and Elisabeth Kappelmann for their excellent technical assistance and Dr Alexander Yassouridis for his help with the statistical analysis.

## References

1. Besedovsky HO, del Rey A. Immune–neuro-endocrine interactions: facts and hypotheses. Endocr Rev 1996;17:64–102.
2. Mason D, MacPhee I, Antoni F. The role of the neuroendocrine system in determining genetic susceptibility to experimental allergic encephalomyelitis in the rat. Immunology 1990;70:1–5.
3. Bolton C, O'Neill JK, Allen SJ, Baker D. Regulation of chronic relapsing experimental allergic encephalomyelitis by endogenous and exogenous glucocorticoids. Int Arch Allergy Immunol 1997;114:74–80.
4. MacPhee IAM, Antoni FA, Mason DW. Spontaneous recovery of rats from experimental allergic encephalomyelitis is dependent on regulation of the immune system by endogenous adrenal corticosteroids. J Exp Med 1989;169:431–445.
5. Heuser I, Yassouridis A, Holsboer F. The combined dexamethasone/CRH test: a refined laboratory test for psychiatric disorders. J Psychiatr Res 1994;28:341–356.
6. Katz D, Taubenberger JK, Cannella B, et al. Correlation between magnetic resonance imaging findings and lesion development in chronic, active multiple sclerosis. Ann Neurol 1993;34:661–669.
7. Miller DH, Thompson AJ, Morrissey SP, et al. High dose steroids in acute relapses of multiple sclerosis: MRI evidence for a possible mechanism of therapeutic effect. J Neurol Neurosurg Psychiatry 1992;55:450–453.

8. Then Bergh F, Kümpfel T, Grasser A, et al. Combined treatment with corticosteroids and moclobemide favors normalization of hypothalamo–pituitary–adrenal axis dysregulation in relapsing–remitting multiple sclerosis. J Clin Endocrinol Metab 2001;86:1610–1615.
9. Roberts N, Barbosa S, Blumhardt LD, et al. Stereological estimation of the total volume of MR visible brain lesions in patients with multiple sclerosis. MAGMA 1994;2:375–378.
10. Dowdell KC, Gienapp IE, Stuckman S, et al. Neuroendocrine modulation of chronic relapsing experimental autoimmune encephalomyelitis: a critical role for the hypothalamic–pituitary–adrenal axis. J Neuroimmunol 1999;100:243–251.
11. Stefferl A, Linington C, Holsboer F, Reul JMHM. Susceptibility and resistance to experimental allergic encephalomyelitis: relationship with hypothalamic–pituitary–adrenocortical axis responsiveness in the rat. Endocrinology 1999;140:4932–4938.
12. Zivadinov R, Rudick RA, De Masi R, et al. Effects of IV methylprednisolone on brain atrophy in relapsing–remitting MS. Neurology 2001;57:1239–1247.
13. Wei T, Lightman SL. The neuroendocrine axis in patients with multiple sclerosis. Brain 1997;120:1067–1076.
14. Giovannoni G, Thorpe JW, Kidd D, et al. Soluble E-selectin in multiple sclerosis: raised concentrations in patients with primary progressive disease. J Neurol Neurosurg Psychiatry 1996; 60:20–26.
15. Fassbender K, Schmidt R, Mössner R, et al. Mood disorders and dysfunction of the hypothalamic–pituitary–adrenal axis in multiple sclerosis. Arch Neurol 1998;55:66–72.
16. Then Bergh F, Kümpfel T, Trenkwalder C, et al. Dysregulation of the hypothalamo–pituitary–adrenal axis is related to the clinical course of MS. Neurology 1999;53:772–777.
17. Trapp BD, Peterson J, Ransohoff RM, et al. Axonal transection in the lesions of multiple sclerosis. N Engl J Med 1998;338: 278–285.
18. Harbuz MS, Rees RG, Eckland D, et al. Paradoxical responses of hypothalamic corticotropin-releasing factor (CRF) messenger ribonucleic acid (mRNA) and CRF-41 peptide and adenohypophysial proopiomelanocortin mRNA during chronic inflammatory stress. Endocrinology 1992;130:1394–1400.
19. Sheline YI. 3D MRI studies of neuroanatomic changes in unipolar major depression: the role of stress and medical comorbidity. Biol Psychiatry 2000;48:791–800.
20. Holsboer F, Grasser A, Friess E, Wiedemann K. Steroid effects on central neurons and implications for psychiatric and neurological disorders. Ann N Y Acad Sci 1994;746:345–359.
21. McFarland HF, Frank JA, Albert PS, et al. Using gadolinium-enhanced magnetic resonance imaging lesions to monitor disease activity in multiple sclerosis. Ann Neurol 1992;32: 758–766.
22. Simon JH, Jacobs LD, Campion MK, et al. A longitudinal study of brain atrophy in relapsing multiple sclerosis. Neurology 1999;53:139–148.
23. Smith ME, Stone LA, Albert PS, et al. Clinical worsening in multiple sclerosis is associated with increased frequency and area of gadopentetate dimeglumine-enhancing magnetic resonance imaging lesions. Ann Neurol 1993;33:480–489.

# Striatal Monoaminergic Terminals in Lewy Body and Alzheimer's Dementias

Masahiko Suzuki, MD, PhD,[1,3,5] Timothy J. Desmond, MS,[3] Roger L. Albin, MD,[2,4] and Kirk A. Frey, MD, PhD[1–3]

**Vesicular monoamine transporter type 2 and benzodiazepine binding site expressions were examined with quantitative autoradiography in postmortem striata from 19 patients with dementia with Lewy bodies, seven patients with dementia with Lewy bodies and Alzheimer's disease, 12 patients with Alzheimer's disease, and eight neurologically normal subjects. Striatal vesicular monoamine transporter type 2 expression in dementia with Lewy bodies and in dementia with Lewy bodies plus Alzheimer's disease was reduced significantly, indicating degeneration of nigrostriatal projections. Striatal benzodiazepine binding site expression was unchanged, indicating preserved intrinsic striatal neuropil. Vesicular monoamine transporter type 2 and benzodiazepine binding site expressions were each preserved in Alzheimer's disease striatum. We conclude that dementia with Lewy bodies may be distinguished from Alzheimer's disease by postmortem examination or by future in vivo measurements of the striatal vesicular monoamine transporter type 2.**

Ann Neurol 2002;51:767–771

Dementia with Lewy bodies (DLB) is characterized clinically by dementia, parkinsonism, fluctuating mental status, dopamine antagonist sensitivity, and recurrent visual hallucinations.[1] DLB is confirmed pathologically by the detection of neurodegeneration in both forebrain and brainstem regions with the accompanying expression of Lewy bodies.[1] DLB may be the second most common form of dementia in the developed world. Parkinsonism may appear also in Alzheimer's disease (AD),[2,3] and the clinical differentiation of DLB and AD remains imprecise. It is suggested that imaging methods visualizing dopaminergic terminals may be

From the Departments of [1]Radiology, (Nuclear Medicine) and [2]Neurology, and [3]Mental Health Research Institute, University of Michigan, Ann Arbor, MI; [4]Geriatrics Research, Education and Clinical Center, Ann Arbor, MI; and [5]Department of Neurology, Jikei University, School of Medicine, Tokyo, Japan.

Received May 21, 2001, and in revised form January 17, 2002. Accepted for publication January 22, 2002.

Published online May 3, 2002, in Wiley InterScience (www.interscience.wiley.com). DOI: 10.1002/ana.10186

Address correspondence to Dr Frey, Room B1G-412/0028 AGH, 1500 East Medical Center Drive, Ann Arbor, MI 48109-0028. E-mail: kfrey@umich.edu

 

useful in differentiating DLB and AD.[4,5] There are, however, discrepant reports of nigrostriatal abnormalities in AD. Some neuroimaging studies report little or no loss of dopamine terminals in AD,[6] but others report reduced striatal dopamine uptake.[4,7] Some postmortem studies report normal substantia nigra neuron numbers and striatal dopamine concentrations in AD, but there are some observations of a reduced substantia nigra neuron number in AD,[8] and parkinsonism in AD may be associated with substantia nigra neurofibrillary tangles (NFTs).[3,9] Discrepant reports may reflect heterogeneity in subject selection, including the possible clinical classification of DLB subjects as AD.

We assessed the integrity of striatal dopamine terminals in neuropathologically defined DLB and AD with in vitro autoradiography of [$^3$H]methoxytetrabenazine binding to vesicular monoamine transporter type 2 (VMAT2).[10,11] As a measure of the intrinsic striatal neuron integrity, we assessed [$^3$H]flumazenil binding to the γ-aminobutyric acid A receptor benzodiazepine binding site.

## Materials and Methods

All brains were obtained from the Michigan Alzheimer's Disease Research Center Brain Bank. Control subject brains with no neurological or psychiatric diseases were obtained from the University of Michigan Hospital autopsy service. After collection, brains were removed, the hemispheres were divided, and 1 to 2cm coronal slabs were cut from one hemisphere. Slabs were frozen rapidly over liquid nitrogen vapor, sealed in plastic to prevent desiccation, and stored at −70°C. The contralateral hemispheres were fixed and processed for routine neuropathological examination. Neuronal plaques and tangles were detected with Bielschowsky's silver stain. Lewy bodies were detected with immunohistochemistry with antisera directed against ubiquitin and α-synuclein. Classification as DLB, AD, or DLB+AD was made on the basis of recent neuropathological consensus criteria.[12,13] Estimates of Lewy body, senile plaque (SP), and NFT density were made by the averaging of counts from four representative 1mm$^2$ fields (20× objective) from each of five different regions in 8μm-thick paraffin-embedded sections. Representative regions included the entorhinal cortex, hippocampus, amygdala, cingulate cortex, and parietal cortex.

Frozen slabs were warmed to −20°C; blocks of relevant regions were cut and coated with an embedding medium to prevent desiccation and were refrozen in crushed dry ice. Blocks were prepared at the level of the head of the caudate, anterior putamen, and nucleus accumbens and at the level of the posterior putamen, including the globus pallidus (Fig 1). Blocks were stored in sealed plastic bags at −70°C until sectioning. Blocks were sectioned coronally on a cryostat microtome at −20°C. Pairs of adjacent 20μm-thick sections were thaw-mounted on poly(L-lysine)-subbed microscope slides and air-dried. Slides were stored at −70°C until use. VMAT2 and benzodiazepine binding site expressions were assayed with [$^3$H]methoxytetrabenazine and [$^3$H]flumazenil, respectively, as described previously.[10,11,14] Autoradiograms were analyzed with video-assisted densitometry (MCID M5 System, Imaging Research, St. Catherines, Ontario, Canada), with calibrated plastic standards for the conversion of film density to apparent tissue radioactivity levels. Statistical comparisons were made with *t* tests with Bonferroni correction for multiple comparisons at an adjusted significance level of $p < 0.01$.

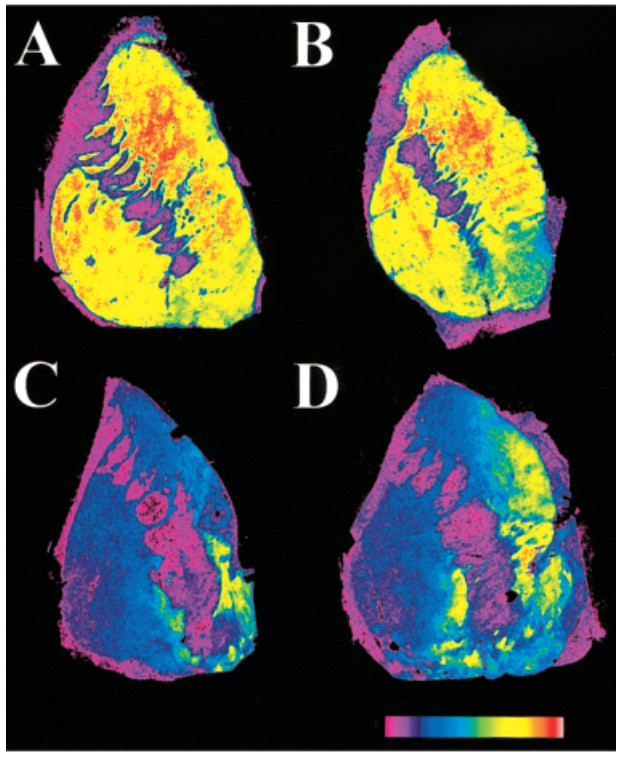


*Fig 1. Autoradiographs of striatal [$^3$H]methoxytetrabenazine ([$^3$H]MTBZ) binding to vesicular monoamine transporter type 2 (VMAT2). Images depict representative examples of VMAT2 patterns and densities in coronal sections at the rostral striatal level in (A) normal subjects, (B) patients with Alzheimer's disease (AD), (C) patients with dementia with Lewy bodies (DLB), and (D) patients with DLB+AD. The autoradiographic film density was transformed to a pseudocolor scale according to the key at the lower right of the image, with red depicting the highest level of binding and violet the lowest. Note the essentially normal striatal binding in AD and the severe losses of VMAT2 binding in both DLB and DLB+AD. In the latter cases, a rim of preserved VMAT2 is consistently observed in the ventral striatum proximate to the internal capsule (C,D).*

## Results

Brains were obtained from 19 DLB patients (average age, 80 years; SD, 6; range, 71–88 years; men, 12; women, 7), 7 DLB+AD patients (average age, 77 years; SD, 5; range, 69–83 years; men, 4; women, 3), 12 AD patients (average age, 80 years; SD, 5; range, 71–87 years; men, 6; women, 6), and 8 controls (av-

*Table. Basal Ganglia Synaptic Markers*

| | Caudate | Anterior Putamen | Posterior Putamen | Globus Pallidus |
|---|---|---|---|---|
| Vesicular monoamine transporter type 2 binding | | | | |
| NC | 98 ± 19 | 106 ± 21 | 117 ± 24[a] | 9 ± 3[a] |
| AD | 79 ± 22 | 88 ± 21 | 97 ± 27 | 9 ± 2 |
| DLB | 16 ± 10[b,f,i] | 35 ± 16[b,f,i] | 13 ± 12[c,f,i] | 6 ± 3[c,g] |
| DLB + AD | 21 ± 18[a,f,h] | 35 ± 27[a,e,g] | 38 ± 18[d] | 8 ± 4 |
| Benzodiazepine binding site | | | | |
| NC | 317 ± 55 | 363 ± 41 | 252 ± 31[a] | 147 ± 18[a] |
| AD | 355 ± 40 | 420 ± 36 | 282 ± 40 | 188 ± 37 |
| DLB | 326 ± 47[b] | 380 ± 62[b] | 280 ± 29[c] | 185 ± 24[c,d] |
| DLB + AD | 356 ± 45[a] | 419 ± 48[a] | 308 ± 41 | 211 ± 27[d] |

All values are expressed as femtomoles per milligram protein and represent mean ±SD of 8 control subjects, 12 AD, 7 DLB + AD, and 19 DLB patients, except where otherwise noted: [a]n = 6. [b]n = 18. [c]n = 17.

Statistical significance (Student's two-tailed *t*-test) after Bonferroni correction for 16 parallel comparisons: [d]$p < 0.05$; [e]$p < 0.01$; [f]$p < 0.001$ vs control; [g]$p < 0.05$; [h]$p < 0.01$, [i]$p < 0.001$ vs AD.

NC = normal control; AD = Alzheimer's disease; DLB = dementia with Lewy bodies.

erage age, 75 years; SD, 10; range, 54–85 years; men, 3; women, 5). The postmortem delay time was 7 ± 3 hours for DLB, 8 ± 2 hours for DLB+AD, 7 ± 3 hours for AD, and 19 ± 6 hours for control subjects. Prior studies in our laboratory indicated minimal effects on benzodiazepine or VMAT2 binding over a simulated 24-hour postmortem delay interval.[15] In DLB, Lewy body density averaged 13 per field, SP density was 16 per field, and NFT density was three per field. There were eight DLB cases with no or virtually no SPs or NFTs. In DLB+AD, Lewy body density averaged 14 per field, SP density was 41 per field, and NFT density was 31 per field. In AD, SP density was 54 per field, and NFT density was 51 per field.

VMAT2 expression was markedly reduced in all striatal subregions in both DLB and DLB+AD (Table; see Fig 1). The magnitude of VMAT2 reduction was considerable, approximately 70 to 90%, comparable across striatal subregions, and similar between DLB and DLB+AD. There was no difference between DLB subjects with or without SPs (Fig 2). In DLB specimens, there was a consistently spared region of [$^3$H]methoxytetrabenazine binding in the ventral striatal complex (see Fig 1). In AD, VMAT2 expression was comparable to that of controls. Benzodiazepine binding site expression was essentially normal in all striatal subregions and was modestly increased in the lateral globus pallidus in DLB, DLB+AD, and AD.

## Discussion

Our results demonstrate marked nigrostriatal dopaminergic projection neuron losses in DLB and DLB+AD, but not in AD. VMAT2 binding is an excellent measure of nigrostriatal terminal integrity because striatal VMAT2 expression is not affected by manipulations that alter synaptic dopamine physiology[11] and striatal VMAT2 binding is a linear function of substantia nigra pars compacta neuron density.[10] Results similar to ours were reported previously with [$^3$H]mazindol binding to the plasmalemmal dopamine transporter (DAT) as a marker of nigrostriatal dopamine terminals.[16] There are, however, differences between these results and the previous report. The previous report describes diminished dopamine terminals in the posterior putamen in DLB but not consistently in other striatal subregions.[16] A marked rostrocaudal gradient of DAT expression was reported in control specimens with a 50% increase in [$^3$H]mazindol binding from caudate to posterior putamen. We find a more modest rostrocaudal gradient, approximately 15%, in

*Fig 2. Caudate nucleus vesicular monoamine transporter type 2 (VMAT2) binding in individual subjects: control (open circles), Alzheimer's disease (AD; open diamonds), dementia with Lewy bodies (DLB) with senile plaque (SP; open, upward-pointing triangles), DLB without SP (filled, upward-pointing triangles), and AD+DLB (open, downward-pointing triangles).*

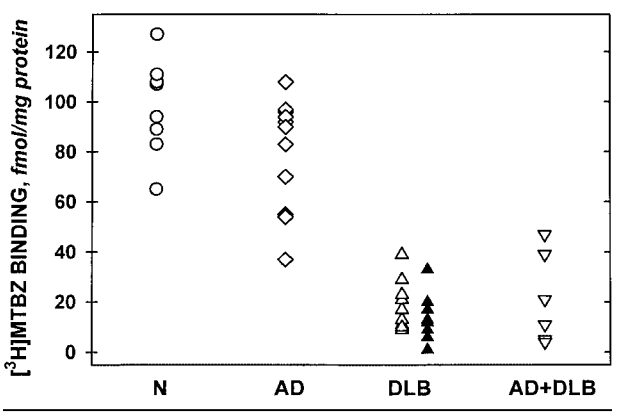

our control specimens (see Table). The earlier study estimated the rostrocaudal DAT binding profile by averaging across subjects with variable individual representations. Therefore, of the 20 total control subjects reported previously, at most 9, and as few as 4, contributed to measures at individual rostrocaudal levels. The previous study's inability to detect diminished anterior striatal DAT expression in DLB may, therefore, reflect anomalously low control DAT binding in the anterior striata rather than their relative sparing in DLB. Prior morphological data support the idea that DLB should be accompanied by the depletion of caudate dopamine terminals. For example, there is a strong correlation between neuronal depletion in the medial substantia nigra, a subregion expected to project to the caudate, and the magnitude of cognitive impairment in demented Parkinson's disease (PD) subjects.[17]

The earlier study of DAT binding also included a PD comparison group and concluded that the magnitude of nigrostriatal terminal loss was greater in PD than DLB.[16] We find marked reductions in nigrostriatal terminal density, comparable to those described in PD, in all dorsal striatal subregions. A possible cause for this apparent discrepancy is case ascertainment. In the previous study, DLB and PD were distinguished on clinical grounds, even though some of the latter subjects probably had dementia, and the pathological findings were similar. Our DLB subjects are defined pathologically and include subjects presenting initially either with parkinsonism or with dementia. We also included a group with both DLB and AD by present pathological criteria. Nigrostriatal terminal loss in this group is identical to that found in DLB.

Spared nucleus accumbens [$^{3}$H]mazindol binding in both DLB and PD was reported previously, but the distribution of residual nucleus accumbens binding was not described in detail.[16] The previous result likely correlates with our identification of a spared subregion of the ventral striatal complex, including parts of the nucleus accumbens. Another study did not describe this spared area of DAT expression in PD.[18] By contrast, an VMAT2 immunohistochemical study of a small series of PD subject brains describes results identical to ours.[19] Spared ventrial striatal dopamine terminals probably arise from relatively rostral medial and medioventral midbrain dopaminergic neurons, described as spared relatively in PD.[20]

DLB and AD have different natural histories and responses to treatment. Clinical differentiation remains imprecise, highlighting the need for diagnostic tests designed to distinguish these two common causes of dementia. In vivo imaging of striatal dopamine terminals may fulfill this need. Metabolic imaging with [$^{18}$F]-2-fluorodeoxyglucose has been proposed also as a means of distinguishing AD and DLB.[21,22] [$^{18}$F]-2-fluorodeoxyglucose studies report occipital hypometabolism as a marker of DLB, but with this method there is some overlap between AD and DLB, degrading diagnostic sensitivity.[22] Our in vitro data indicate reliable separation of DLB and AD. Positron emission tomography or single-photon emission computed tomography methods targeting striatal dopamine terminals may have sufficient sensitivity and specificity to be useful clinically. A combination of [$^{18}$F]-2-fluorodeoxyglucose and dopaminergic imaging may also permit differentiation of DLB from PD. The latter shows relative sparing of caudate dopamine terminals, whereas the former should display posterior cingulate and associated neocortical metabolic changes.[22]

These studies were supported by United States Public Health Service grants from the National Institute of Aging (AG08671, K.A.F.) and the National Institute for Neurological Disorders and Stroke (NS38166, R.L.A.) and by a Veteran's Administration merit review grant (R.L.A.).

## References

1. Brown DF. Lewy body dementia. Ann Med 1999;31:188–196.
2. Lopez OL, Wisniewski SR, Becker JT, Boller F, DeKosky ST. Extrapyramidal signs in patients with probable Alzheimer disease. Arch Neurol 1997;54:969–975.
3. Liu Y, Stern Y, Chun MR, et al. Pathological correlates of extrapyramidal signs in Alzheimer's disease. Ann Neurol 1997;41: 368–374.
4. Walker Z, Costa DC, Ince P, et al. In-vivo demonstration of dopaminergic degeneration in dementia with Lewy bodies. Lancet 1999;354:646–647.
5. Donnemiller E, Heilmann J, Wenning GK, et al. Brain perfusion scintigraphy with $^{99m}$Tc-HMPAO or $^{99m}$Tc-ECD and $^{123}$I-β-CIT single-photon emission tomography in dementia of the Alzheimer-type and diffuse Lewy body disease. Eur J Nucl Med 1997;24:320–325.
6. Tyrrell PJ, Sawle GV, Ibanez V, et al. Clinical and positron emission tomographic studies in the "extrapyramidal syndrome" of dementia of the Alzheimer type. Arch Neurol 1990;47: 1318–1323.
7. Rinne JO, Sahlberg N, Ruottinen H, et al. Striatal uptake of the dopamine reuptake ligand [$^{11}$C]-β-CFT is reduced in Alzheimer's disease assessed by positron emission tomography. Neurology 1998;50:152–156.
8. Kazee AM, Cox C, Richfield EK. Substantia nigra lesions in Alzheimer disease and normal aging. Alzheimer Dis Assoc Disord 1995;9:61–67.
9. Perry RH, Irving D, Blessed G, et al. Senile dementia of Lewy body type. A clinically and neuropathologically distinct form of Lewy body dementia in the elderly. J Neurol Sci 1990;95: 119–139.
10. Vander Borght TM, Sima AAF, Kilbourn MR, et al. [$^{3}$H]Methoxytetrabenazine: a high specific activity ligand for estimating monoaminergic neuronal integrity. Neuroscience 1995;68:995–962.
11. Vander Borght TM, Kilbourn MR, Desmond TJ, et al. The vesicular monoamine transporter is not regulated by dopaminergic drug treatments. Eur J Pharmacol 1995;294:575–584.
12. McKeith IG, Galasko D, Kosaka K, et al. Consensus guidelines for the clinical and pathologic diagnosis of dementia with Lewy bodies (DLB): report of the consortium on DLB international workshop. Neurology 1996;47:1113–1124.

13. Anonymous. Consensus recommendations for the postmortem diagnosis of Alzheimer's disease. The National Institute on Aging and Reagan Institute working group on diagnostic criteria for neuropathologic assessment of Alzheimer's disease. Neurobiol Aging 1997;18:S1–S2.
14. Burdette DE, Sakurai SY, Henry TR, et al. Temporal lobe central benzodiazepine binding in unilateral mesial temporal lobe epilepsy. Neurology 1995;45:934–941.
15. Suzuki M, Desmond TJ, Albin RL, Frey KA. Vesicular neurotransmitter transporters in Huntington's disease: initial observations and comparison with traditional synaptic markers. Synapse 2001;41:329–336.
16. Piggott MA, Marshall EF, Thomas N, et al. Striatal dopaminergic markers in Lewy bodies, Alzheimer's and Parkinson's diseases: rostrocaudal distribution. Brain 1999;122:1449–1468.
17. Rinne JO, Rummukainen J, Paljarvi L, Rinne UK. Dementia in Parkinson's disease is related to neuronal loss in the medial substantia nigra. Ann Neurol 1989;26:47–50.
18. Murray AM, Weihmueller FB, Marshall JF, et al. Damage to dopamine systems differs between Parkinson's disease and Alzheimer's disease with parkinsonism. Ann Neurol 1995;37:300–311.
19. Miller GW, Erickson JD, Perez JT, et al. Immunochemical analysis of vesicular monoamine transporter (VMAT2) protein in Parkinson's disease. Exp Neurol 1999;156:138–148.
20. Damier P, Hirsch EC, Agid Y, Graybiel AM. The substantia nigra of the human brain II: Patterns of loss of dopamine-containing neurons in Parkinson's disease. Brain 1999;122:1437–1448.
21. Albin RL, Minoshima S, D'Amato C, et al. Fluorodeoxyglucose positron emission tomography in diffuse Lewy body disease. Neurology 1996;47:462–466.
22. Minoshima S, Foster NL, Sima AAF, et al. Alzheimer's disease versus dementia with Lewy bodies: cerebral metabolic distinction with autopsy confirmation. Ann Neurol 2001;50:358–365.

# Human Herpesvirus 6 Encephalitis Associated with Hypersensitivity Syndrome

Yasuhiro Fujino, MD, Masashi Nakajima, MD, Hirosato Inoue, MD, Tomohiko Kusuhara, MD, and Tatsuo Yamada, MD

**Hypersensitivity syndrome, a serious systematic reaction to a limited number of drugs, is associated with the reactivation of human herpesvirus 6. A 56-year-old man developed acute limbic encephalitis followed by multiple organ failure during the course of toxic dermatitis induced by aromatic anticonvulsants. The clinical features of skin eruptions, high fever, eosinophilia, and atypical lymphocytosis were compatible with drug hypersensitivity syndrome. The patient showed seroconversion for human herpesvirus 6, and polymerase chain reaction detected human herpesvirus 6 DNA in the cerebrospinal fluid. To our knowledge, this is the first report of human herpesvirus 6 encephalitis associated with hypersensitivity syndrome.**

Ann Neurol 2002;51:771–774

Systemic and possibly fatal hypersensitivity reactions to phenytoin have long been recognized.[1] They are characterized by fever, pleomorphic eruption, lymphadenopathy, eosinophilia, atypical lymphocytosis, hepatitis, and multiple organ failure. Such adverse reactions have been reported after the use of aromatic anticonvulsants, sulfasalazine, allopurinol, dapsone, minocycline, sodium valproate, and ethosuximide. Some recent reports suggest that the reactivation of human herpesvirus 6 (HHV-6) may contribute to the development of drug hypersensitivity syndrome.[2–6] Primary HHV-6 infection is associated with exanthem subitum and febrile illness in children.[7] HHV-6 recently has been recognized as an opportunistic pathogen causing limbic encephalitis in persons infected with human immunodeficiency virus and in transplant recipients.[7–13] We report a patient with limbic encephalitis associated with the presence of the HHV-6 genome in the cere-

From the Department of Neurology, School of Medicine, Fukuoka University, Fukuoka, Japan.

Received Nov 1, 2001, and in revised form Dec 18. Accepted for publication Feb 5, 2002.

Published online May 3, 2002, in Wiley InterScience (www.interscience.wiley.com). DOI: 10.1002/ana.10194

Address correspondence to Dr Nakajima, Department of Neurology, School of Medicine, Fukuoka University, 7-45-1 Nanakuma, Johnan-ku, Fukuoka, Japan 814-0180.
E-mail: masashi@fukuoka-u.ac.jp

 

brospinal fluid (CSF) during the course of hypersensitivity syndrome.

## Case Report

A 56-year-old hypertensive man developed generalized erythematous macules after taking 134mg of phenytoin and 66mg of phenobarbital daily for 3 weeks. He had had a late-onset, generalized convulsion of unknown cause 6 months previously. A computed tomography scan of the head had shown lacunae in the centrum semiovale on both sides. Routine hematological and laboratory tests, as well as an electroencephalogram after the seizure, were unremarkable. He had been prescribed 600mg of sodium valproate daily but continued to have seizures once a month, although he was well during the interictal periods.

The erythematous macules prompted his physician to withdraw all the antiepileptics, and resolution of the macules began. Within a week, however, he came down with a high-grade fever of 39.8°C and generalized erythroderma and edema. Laboratory studies showed a white blood cell count of $23.3 \times 10^9$/L (23% eosinophils and 9.5% atypical lymphocytes) and abnormal liver function results. A skin biopsy showed a spongiotic epidermis with liquefactive degeneration of the epidermal basal layer. Epidermal and perivascular dermal infiltrates with lymphocytes were present, some of them transformed, as well as a few eosinophils. A daily dose of 30mg of oral prednisone gradually ameliorated his fever and laboratory abnormalities, but the next week he had a generalized convulsion and mild postictal confusion that lasted for a few days. That was followed by fever, disorientation, and right hemiparesis.

On examination, he had generalized edema and erythroderma with marked desquamation, which was worst in the face. He responded orally to simple commands but tended to be unresponsive and occasionally had roving eye movements. Brainstem reflexes were well preserved. Flaccid right hemiparesis with bilateral extensor plantar responses was present. A hemogram showed leukocytosis with neither eosinophils nor atypical lymphocytes. His platelet count was decreased. Liver dysfunction was in relapse, and creatinine clearance was 18ml/min. Metabolic causes of encephalopathy were ruled out. Serum levels of immunoglobulins and complements were normal. A computed tomography scan of the head was unremarkable. Lumbar puncture showed an opening pressure of 220mm $H_2O$, a mononuclear pleocytosis of 43 cells/μl, a protein level of 106mg/dl, and a glucose level of 72mg/dl. Bacterial and fungal smears, cultures, and antigens were all negative.

Under the presumptive diagnosis of herpes simplex encephalitis, acyclovir (20mg/kg/day) was started, but within 2 days the patient's neurological condition had deteriorated to coma and central hypoventilation. He experienced frequent partial seizures involving the right face and arm, and he had secondary generalization. These seizures were controlled by the intravenous administration of diazepam. An electroencephalogram showed diffuse, slow waves with an occasional solitary spike and waves in the left frontal and temporal leads without periodic patterns. Magnetic resonance imaging of the head showed bilateral lesions involving the amygdala, medial temporal lobe, insula, and cingulate gyrus (Fig 1). A 10-day course of acyclovir resulted in a decrease in CSF cells but no clinical improvement. He developed multiple organ failure and died 18 days after the onset of coma and 5 weeks after the onset of the macular rashes. Autopsy was refused. His clinical course is summarized in a timeline (Fig 2).

### *Virological and Serological Studies*

Acute-phase serum and CSF samples were drawn on the day of the neurological examination. Both the acute-phase samples and the serum samples taken 2 weeks later were tested for antibodies to herpes simplex virus types 1 (HSV-1) and 2 (HSV-2), herpes zoster virus, HHV-6, cytomegalovirus, and Epstein-Barr virus, as well as antibodies to Japanese encephalitis, measles, rubella, coxsackie B4, influenza A and B, and mumps. Of these viruses, HHV-6 immunoglobulin G (IgG) antibody titers had increased from 80 to 640 in the fluorescent antibody test. HHV-6 fluorescent antibody immunoglobulin M antibodies were negative in the acute-phase serum specimen. IgG antibodies to HSV-1 and 2, herpes zoster virus, cytomegalovirus, Epstein-Barr virus, measles, ru-

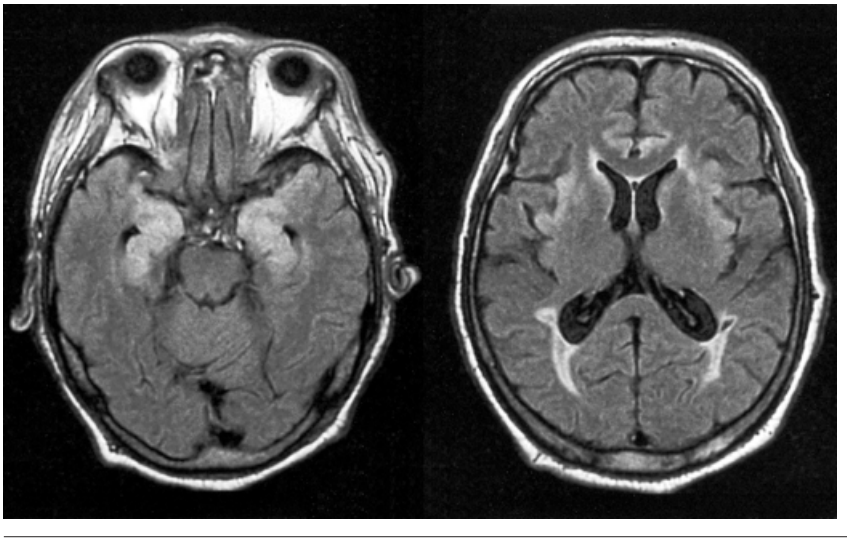

*Fig 1. Fluid-attenuated inversion recovery sequence magnetic resonance imaging (MRI) shows bilateral hyperintensity of the gray matter involving the amygdala, medial temporal lobe, insula, and cingulate gyrus. The right side of each image corresponds to the left side of the brain.*

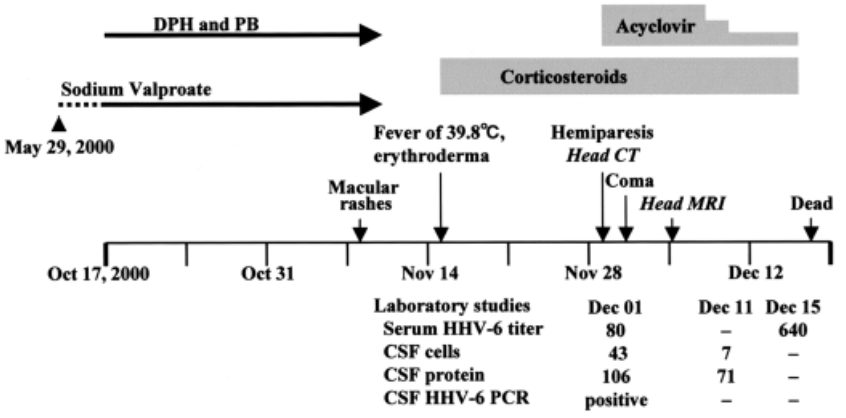


*Fig 2. Clinical course and laboratory studies. The timeline has a scale in weeks. Vertical arrows indicate the onset of symptoms and the dates of radiological examinations. DPH = diphenylhydantoin; PB = phenobarbital; CT = computed tomography; MRI = magnetic resonance imaging; CSF = cerebrospinal fluid; HHV-6 = human herpesvirus 6; dash = not done.*

bella, and mumps were all positive but showed no seroconversion. Serum titers of the other viruses were negative in both samples. Both the acute-phase CSF specimen and the CSF specimen taken 10 days later showed negative immunoglobulin M and IgG antibody titers for HSV-1 and HHV-6. The polymerase chain reaction analysis performed with DNA extracted from the acute-phase CSF specimen was positive for HHV-6 and negative for HSV-1. The patient was seronegative for human immunodeficiency virus types 1 and 2.

## Discussion

Our patient developed macular rashes that evolved into erythroderma 3 weeks after the administration of aromatic anticonvulsants. This incubation period and the clinical features strongly support the diagnosis of drug hypersensitivity syndrome.[2–6] Our patient's hypersensitivity syndrome was followed by acute limbic encephalitis and also by seroconversion for HHV-6 and its DNA in the CSF. HHV-6 may be harbored in the normal human brain after primary infection.[14] Detection of HHV-6 DNA in the CSF, however, is considered a reliable diagnostic tool for HHV-6 encephalitis.[13,15] HHV-6, like HSV-1, has a propensity to infect the limbic system. Drobyski and colleagues,[8] using HHV-6-specific antibodies, immunohistochemically detected HHV-6-infected glias and neurons distinctively in the frontal lobe and hippocampal gyrus in a bone marrow transplant recipient who died of encephalitis. In subsequent reports of HHV-6 encephalitis diagnosed on polymerase chain reaction detection of HHV-6 DNA in the CSF, magnetic resonance imaging results were abnormal in 6 of 20 patients. Three of the 6 patients showed bilateral, symmetrical involvement of the medial temporal lobe or limbic system,[10–12] which resembled the findings for our patient. Although we could not detect fluorescent antibodies to HHV-6 in the CSF, the positive genome in the CSF and the magnetic resonance imaging findings support the diagnosis of HHV-6 encephalitis.

Persistent or latent HHV-6 infection of the central nervous system, if it is possible, could have been the cause of our patient's repeated, generalized convulsions before the onset of hypersensitivity syndrome, but there are no available data to support this hypothesis. We believe that in this hypertensive man with multiple lacunae, ischemic brain damage may have caused symptomatic epilepsy. The absence of HHV-6 fluorescent immunoglobulin M antibodies in the acute stage of encephalitis and the increase in IgG antibodies 2 weeks later suggest reactivation of HHV-6 during the course of hypersensitivity syndrome.[4] The association between an isolated rise in anti-HHV-6 IgG antibodies and this syndrome has been reported.[2–6] HHV-6 has been detected in skin lesions in 2 cases.[3,6] In another case, HHV-6 was isolated from peripheral blood mononuclear cells; this is indicative of the presence of an infective form of the virus.[4]

Although the HHV-6 reactivation mechanism in hypersensitivity syndrome is still not known, our patient's limbic encephalitis was linked chronologically to the syndrome and the reactivation of HHV-6. Because clinical diseases caused by HHV-6 are treatable with ganciclovir or foscarnet, both of which are more sensitive than acyclovir,[11,13] this virus should be recognized as a possible cause of acute limbic encephalitis.

## References

1. Haruda F. Phenytoin hypersensitivity: 38 cases. Neurology 1979;29:1480–1485.
2. Descamps V, Bouscarat F, Laglenne S, et al. Human herpesvirus 6 infection associated with anticonvulsant hypersensitivity syndrome and reactive haemophagocytic syndrome. Br J Dermatol 1997;137:605–608.
3. Suzuki Y, Inagi R, Aono T, et al. Human herpesvirus 6 infection as a risk factor for the development of severe drug-induced hypersensitivity syndrome. Arch Dermatol 1998;134:1108–1112.
4. Tohyama M, Yahata Y, Yasukawa M, et al. Severe hypersensitivity syndrome due to sulfasalazine associated with reactivation of human herpesvirus 6. Arch Dermatol 1998;134:1113–1117.
5. Conilleau V, Dompmartin A, Verneuil L, et al. Hypersensitivity syndrome due to 2 anticonvulsant drugs. Contact Dermatitis 1999;41:141–144.

6. Descamps V, Valance A, Edlinger C, et al. Association of human herpesvirus 6 infection with drug reaction with eosinophilia and systemic symptoms. Arch Dermatol 2001;137: 301–304.
7. Kosuge H. HHV-6, 7 and their related diseases. J Dermatol Sci 2000;22:205–212.
8. Drobyski WR, Knox KK, Majewski BS, Carrigan DR. Brief report: fatal encephalitis due to variant B human herpesvirus-6 infection in a bone marrow-transplant recipient. N Engl J Med 1994;330:1356–1360.
9. Knox KK, Carrigan DR. Active human herpesvirus (HHV-6) infection of the central nervous system in patients with AIDS. J Acquir Immune Defic Syndr Hum Retrovirol 1995;9:69–73.
10. Tsujimura H, Iseki T, Date Y, et al. Human herpesvirus-6 encephalitis after bone marrow transplantation: magnetic resonance imaging could identify the involved sites of encephalitis. Eur J Haematol 1998;61:284–285.
11. Bethge W, Beck R, Jahn G, et al. Successful treatment of human herpesvirus-6 encephalitis after bone marrow transplantation. Bone Marrow Transplant 1999;24:1245–1248.
12. Tiacci E, Luppi M, Barozzi P, et al. Fatal herpesvirus-6 encephalitis in a recipient of a T-cell-depleted peripheral blood stem cell transplant from a 3-loci mismatched related donor. Haematologica 2000;85:94–97.
13. Singh N, Paterson D. Encephalitis caused by human herpesvirus-6 in transplant recipients: relevance of a novel neurotrophic virus. Transplant 2000;69:2474–2479.
14. Luppi M, Barozzi P, Maiorana A, et al. Human herpesvirus-6 infection in normal human brain tissue. J Infect Dis 1994;169: 943–944.
15. Wang F-Z, Linde A, Hägglund H, et al. Human herpesvirus 6 DNA in cerebrospinal fluid specimens from allogeneic bone marrow transplant patients: does it have clinical significance? Clin Infect Dis 1999;28:562–568.

# Mitochondrial DNA Nucleotide Changes C14482G and C14482A in the ND6 Gene Are Pathogenic for Leber's Hereditary Optic Neuropathy

Maria Lucia Valentino, MD,[1] Patrizia Avoni, MD,[1] Piero Barboni, MD,[2] Francesco Pallotti, MD, PhD,[3] Chiara Rengo, PhD,[4,5] Antonio Torroni, PhD,[4,6] Marzio Bellan, MD,[1] Agostino Baruzzi, MD,[1] and Valerio Carelli, MD, PhD[1]

**A novel mitochondrial DNA nucleotide transversion, C14482A (M64I), different from the previously reported C14482G (M64I), was found to cause Leber's hereditary optic neuropathy with visual recovery in an Italian family. These equivalent changes are the fifth pathogenic mutation for pure Leber's hereditary optic neuropathy. This confirms that the ND6 gene of complex I is a mutational hot spot and suggests that different amino acid substitutions at residue 64, as induced by C14482G or C14482A (M64I) and the common T14484C (M64V) mutations, are associated with visual recovery.**

Ann Neurol 2002;51:774–778

Leber's hereditary optic neuropathy (LHON) is a maternally inherited degeneration of the retinal ganglion cells that leads to optic atrophy with preferential and prevalent loss of the small fibers serving central vision.[1] Point mutations in mitochondrial DNA (mtDNA), affecting genes encoding complex I subunits, are pathogenic for LHON. In a large majority of LHON cases, one of three prevalent mutations, at positions

From the [1]Dipartimento di Scienze Neurologiche, Università di Bologna, Bologna, Italy; [2]Dipartimento di Oftalmologia, "Centro Salus," Bologna, Italy; [3]Department of Neurology, College of Physicians and Surgeons, Columbia University, New York, NY; [4]Dipartimento di Genetica e Biologia Molecolare, Università di Roma "La Sapienza," Rome, Italy; [5]Istituto di Medicina Legale, Università Cattolica del Sacro Cuore di Roma, Rome, Italy; and [6]Dipartimento di Genetica e Microbiologia, Università di Pavia, Pavia, Italy.

Received Nov 19, 2001, and in revised form Feb 2, 2002. Accepted for publication Feb 2, 2002.

Published online May 3, 2002, in Wiley InterScience (www.interscience.wiley.com). DOI: 10.1002/ana.10193

Address correspondence to Dr Carelli, Dipartimento di Scienze Neurologiche, Università di Bologna, Via Ugo Foscolo 7, 40123 Bologna, Italy. E-mail: carelli@neuro.unibo.it

 

G11778A/ND4, G3460A/ND1, or T14484C/ND6, is found.[1] Recently, a fourth rare pathogenic mutation, A14495G/ND6, was reported in two LHON families.[2] The ND6 subunit is also affected by the pathogenic mutation T14459A, leading to the variant phenotype of LHON/dystonia/Leigh syndrome,[3,4] and by some putative LHON mutations found so far only in a single case or pedigree (C14482G, C14498T, and C14568T).[5,6] Therefore, it has been suggested that the ND6 gene is a hot spot for LHON mutations.[2]

A small subset of patients who received a clinical diagnosis compatible with LHON and presented with maternal inheritance, but lacked the three prevalent pathogenic mutations, have been recognized worldwide. Sequence analysis of candidate regions of mtDNA would be appropriate in these cases, and ND6 represents the best candidate gene. Here we report on one such family in which a new ND6 nucleotide change (C14482A), causal to LHON, was found.

## Patients and Methods

An Italian family with two maternally related affected males was observed (Fig 1). The proband, a 13-year-old boy, suffered a rapid bilateral loss of vision within 1 week (Fig 2A). The left optic nerve (OS) was less affected than the right (OD). The fundus examination showed a hyperemic optic disc and peripapillary telangiectatic vessels. Neurological examination demonstrated that reflexes were diffusely brisk. Cerebral magnetic resonance imaging and cerebrospinal fluid examination were normal, as were extensive investigations for autoimmunity and infection. A search for the LHON mutations G11778A, G3460A, T14484C, and T14459A was negative. Starting from the 3rd month after onset, a progressive recovery of visual acuity and then an improvement in the visual field defect were observed, as detailed in Figure 2B–D.

The proband's maternal uncle had a sudden visual loss in OD at age 10 years, followed a few days later by the involvement of OS. His visual acuity was 20/200 in OD and 20/100 in OS, with a further worsening the following month to 8/200 in OD and 20/200 in OS. According to the patient's interview, visual function started to recover a few weeks later, but no medical documentation of this event is available. However, his current visual acuity at age 28 years is 20/100 in OD and 20/60 in OS. A recent neurological examination showed diffusely brisk reflexes, prevalent in the lower limbs. These two patients were not tobacco smokers or alcohol drinkers at the age of onset, and they had not been exposed to any other obvious risk factor.

*Fig 1. Pedigree of an Italian family carrying the mutation C14482A. Black symbols indicate the affected individuals (the arrow points to the proband). Asterisks indicate the individuals from the maternal line who were available for mitochondrial DNA analysis.*

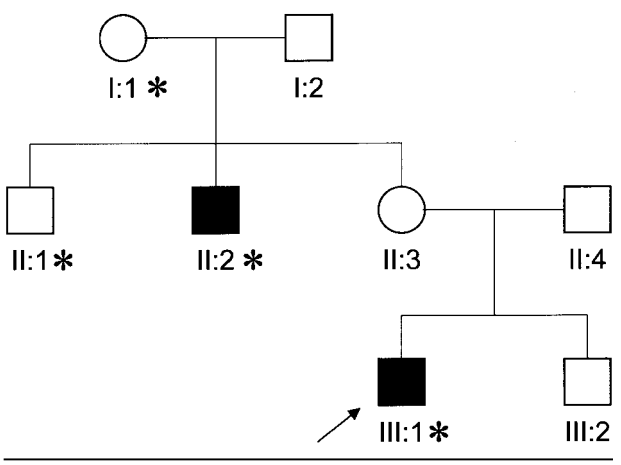


Blood total DNA was extracted by a standard phenol-chloroform method from four maternally related individuals, including the two affected ones (see Fig 1). The ND6 subunit gene was amplified in two fragments by polymerase chain reaction (primers F14130-14152 and R14538-14519 and F14407-14424 and R14705-14682) and sequenced on an ABI PRISM 310 genetic analyzer (Foster City, CA). Restriction fragment length polymorphism analysis of the C14482A mutation was carried out, amplifying a polymerase chain reaction fragment with the primer pair F14459-14481 and R14538-14519. A double mismatch at nucleotides 14477–14478 (GT) in the forward primer creates a *Bst*EII restriction site in the wild-type sequence, which is eliminated by the presence of the C14482A mutation. To evaluate the ratio of mutant to wild-type mtDNA, we ran a last hot cycle in the presence of [$\alpha$-$^{32}$P]dCTP and electrophoresed the *Bst*EII digestion products through a 15% nondenaturing polyacrylamide gel. The *Bst*EII digested fragments were quantified by the scanning of the gel in a PhosphorImager (GS-363; Bio-Rad, Hercules, CA). Sequence analysis of the proband's mtDNA control region (between positions 16,000 and 200) and a restriction fragment length polymorphism survey of haplogroup J markers were performed as previously described.[7]

## Results

The clinical history and inheritance pattern, compatible with maternal transmission, were strongly suggestive of LHON in our patients, who lacked any of the common LHON pathogenic mutations. We decided to sequence the ND6 subunit as the first-choice candidate gene, given the recent reports of LHON mutations clustering in it.[2,5,6] The only nucleotide change relative to the reference sequence[8] was at position 14482, a C-to-A transversion (Fig 3A). This mutation differs from the previously reported C14482G, but it induces the same amino acid change, M64I (in which an isoleucine replaces methionine). The latter is also the same amino acid affected by the common LHON mutation T14484C; however, this mutation induces a different amino acid change, M64V (in which a valine replaces methionine). Restriction fragment length polymorphism analysis showed that both affected individuals and one unaffected maternal relative were homoplasmic for the C14482A mutation, whereas the proband's grandmother was heteroplasmic (see Fig 3B). The C14482A mutation was absent in 100 controls (27 LHON cases carrying

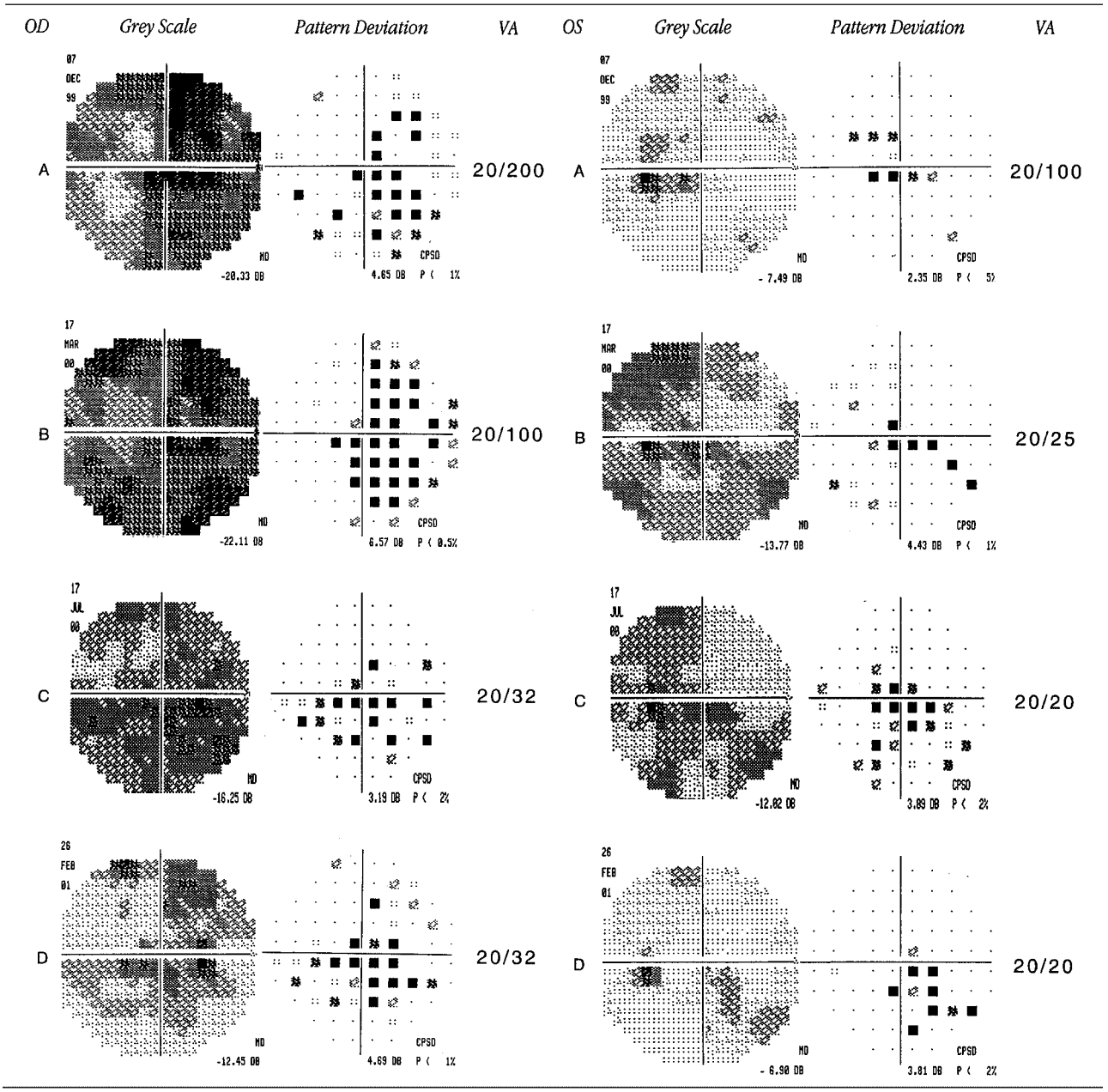


*Fig 2. Full-threshold, 30-degree visual fields (Humphrey field analyzer; Zeiss-Humphrey, Dublin, CA) of the right optic nerve (OD) and left optic nerve (OS) and correspondent visual acuity (VA) follow-up document the progression of visual recovery in the proband. (A) Visual fields and acuity at first observation, 1 week after onset, showed a centrocecal scotoma in OD and a central scotoma in OS. (B) Three months after onset, VA was improved, possibly because of the fenestration of the scotomas, as demonstrated by perimetry. However, a diffuse threshold depression was evident. (C) Seven months after onset, a further dramatic improvement of VA was evident with complete recovery in OS, paralleled by increased sensitivity and some reduction of central scotomas. (D) Fourteen months after onset, stabilized visual acuity was accompanied by a further, consistent increase in sensitivity and restriction of central scotomas.*

one of the three common pathogenic mutations; 27 optic atrophy cases of uncertain cause, some compatible with LHON but negative for the three LHON common pathogenic mutations; and 46 normal controls). Sequencing of the control region showed that the two subjects with the C14482A mutation harbored mtDNA with the following nucleotide changes relative to the reference sequence[8]: C16069T, T16126C, C16261T, A73G, G185A, and A189G. This motif distinguishes haplogroup J mtDNA,[7] thereby indicating that the C14482A family harbored mtDNA belonging to J. This classification was further confirmed by the finding that the mtDNA also harbored +4216 *Nla*III, +10394 *Dde*I, −13704 *Bst*OI, +15254 *Acc*I, and +15812 *Rsa*I,

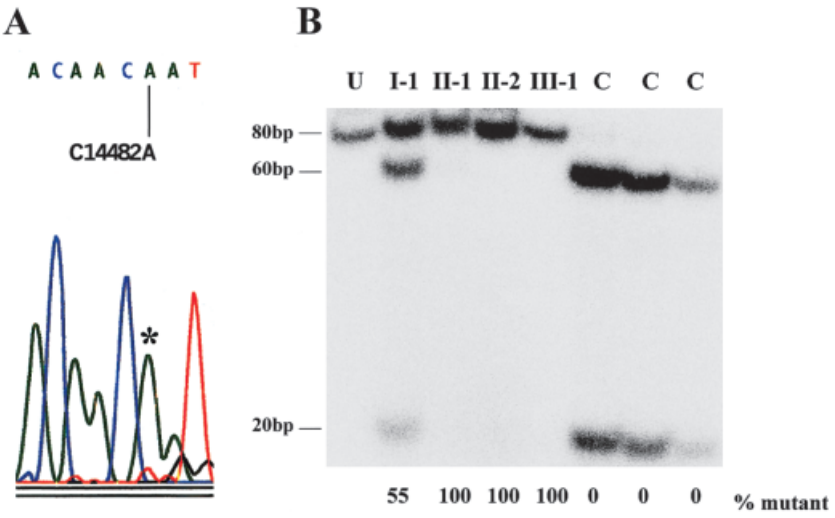


*Fig 3. Molecular investigations. (A) Sequence analysis shows the mutation C14482A in the proband. (B) Restriction fragment length polymorphism analysis shows the segregation of the mutation C14482A in 4 maternally related individuals from the Italian family (U = uncut polymerase chain reaction product, C = controls). The mismatch primers introduce a* BstE*II restriction site in the wild-type sequence, resulting in two 60bp and 20bp fragments in normal individuals (controls). The mutation C14482A eliminates this restriction site, resulting in an 80bp fragment equal to the uncut polymerase chain reaction product. The coexistence of three bands (80bp, 60bp, and 20bp) indicates heteroplasmy. The proband's unaffected grandmother (I-1) was heteroplasmic, with 55% mutant C14482A mitochondrial DNA, whereas the unaffected (II-1) and affected individuals (II-2 and III-1) were homoplasmic mutant.*

thereby indicating J1 membership.[9] Thirty additional control individuals from various countries in the Mediterranean area who harbored haplogroup J mtDNA[10] were also screened for the C14482A mutation, but none of them was found to harbor it.

## Discussion

We believe that the C14482A mutation in the ND6 gene of complex I is causal to LHON, for the following four reasons.

First, it affects the very same amino acid, at position 64, as the common LHON mutation T14484C. However, the amino acid change induced by C14482A differs from that induced by T14484C, being M64I instead of M64V. Both isoleucine and valine are hydrophobic and essentially equivalent in replacing methionine, which is also hydrophobic. However, the latter differs substantially with respect to the presence of a sulfur atom. The M64 amino acid position is not highly conserved per se, but it is located within the most conserved region of the ND6 subunit, the hydrophobic and transmembrane helix C.[11] This protein domain is a hot spot for well-established mutations associated with LHON (A14495G)[2] or LHON-related phenotypes (T14459A)[3,4] and for a further putative pathogenic LHON mutation (C14498T).[6] Moreover, at least two of these helix C mutations (T14484C and T14459A) present some functional analogy by inducing an increased sensitivity to productlike inhibitors at the quinol site of complex I.[11,12]

Second, a previous report suggested that a different nucleotide change at the same location (C14482G), found in an LHON family of Turkish origin, was pathogenic.[5] Both C14482G and C14482A induce the same amino acid change, M64I. Therefore, the Italian family is the second in which LHON has been associated with the M64I amino acid change. These equivalent nucleotide changes, C14482G and C14482A, were not found in large cohorts of controls, including sets of haplogroup-matched individuals, and to our knowledge they have never been reported as population polymorphisms.[13]

Third, in both the Turkish and Italian families, the M64I amino acid change was associated with a mild form of LHON consistently characterized by recovery of visual acuity in multiple individuals.[5] This feature resembles very closely the clinical phenotype of LHON associated with the common mutation T14484C,[1] which is also characterized by frequent recovery of visual acuity, particularly when the onset is at a younger age, as in our two patients. This could be due to the similar nature of the amino acids isoleucine and valine replacing methionine at position 64, which most likely induces a similar functional defect of complex I.

Finally, the C14482A mutation was homoplasmic in both our patients, but the proband's grandmother showed heteroplasmy (see Fig 3B). Heteroplasmy is considered an indicator of possible pathogenic significance,[14] even though it is not an absolute requirement

in LHON, as historically shown by the seminal identification of the pathogenic mutation G11778A.[15]

In conclusion, this study shows that a nucleotide change at position 14482 (G or A) should be considered a rarely occurring fifth pathogenic mutation for pure LHON and should be included in diagnostic protocols. Moreover, our analysis suggests that the C14482 (G or A) nucleotide changes are possibly similar, from a prognostic point of view, to the common T14484C mutation. A last observation of interest is that the C14482A mutation was found on a haplogroup J mtDNA background similar to the majority of the T14484C mutations observed in Europeans.[9,16,17] However, the Turkish family with the C14482G mutation belonged to haplogroup I.[5] Therefore, a larger cohort of LHON families with 14482 nucleotide changes is required to determine whether there is a link between these mutations and haplogroup J. In any case, the M64I amino acid substitution was associated with a good prognosis in both the Italian and Turkish families, suggesting that at least this feature is not modulated by the mtDNA haplogroup, as has been previously observed for the mutation T14484C.[1,18]

This work was supported by Fondazione "Gino Galletti" (V.C.) and by Telethon-Italy (E.0890, A.T.)

We thank Dr Mirella Mochi, Dr Anna Ghelli, and Sabrina Farne for their technical help and useful discussions.

## References

1. Carelli V. Leber's hereditary optic neuropathy. In: Schapira AHV, DiMauro S, eds. Mitochondrial disorders in neurology 2. Woburn, MA: Butterworth-Heinemann, 2002:115–142. Blue Books of Practical Neurology; vol 26.
2. Chinnery PF, Brown DT, Andrews RM, et al. The mitochondrial ND6 gene is a hot spot for mutations that cause Leber's hereditary optic neuropathy. Brain 2001;124:209–218.
3. Shoffner JM, Brown MD, Stugard C, et al. Leber's hereditary optic neuropathy plus dystonia is caused by a mitochondrial DNA point mutation. Ann Neurol 1995;38:163–169.
4. Kirby DM, Kahler SG, Freckmann M-L, et al. Leigh disease caused by the mitochondrial DNA G14459A mutation in unrelated families. Ann Neurol 2000;48:102–104.
5. Howell N, Bogolin C, Jamieson R, et al. mtDNA mutations that cause optic neuropathy: how do we know? Am J Hum Genet 1998;62:196–202.
6. Wissinger B, Besch D, Baumann B, et al. Mutation analysis of the ND6 gene in patients with Leber's hereditary optic neuropathy. Biochem Biophys Res Commun 1997;234:511–515.
7. Torroni A, Cruciani F, Rengo C, et al. The A1555G mutation in the 12S rRNA gene of human mtDNA: recurrent origins and founder events in families affected by sensorineural deafness. Am J Hum Genet 1999;65:1349–1358.
8. Anderson S, Bankier AT, Barrell BG, et al. Sequence and organization of the human mitochondrial genome. Nature 1981; 290:457–465.
9. Torroni A, Petrozzi M, D'Urbano L, et al. Haplotype and phylogenetic analyses suggest that one European-specific mtDNA background plays a role in the expression of Leber hereditary optic neuropathy by increasing the penetrance of the primary mutations 11778 and 14484. Am J Hum Genet 1997;60: 1107–1121.
10. Richards M, Macaulay V, Hickey E, et al. Tracing European founder lineages in the Near Eastern mtDNA pool. Am J Hum Genet 2000;67:1251–1276.
11. Carelli V, Ghelli A, Bucchi L, et al. Biochemical features of mtDNA 14484 (ND6/M64V) point mutation associated with Leber's hereditary optic neuropathy. Ann Neurol 1999;45: 320–328.
12. Jun AS, Trounce IA, Brown MD, et al. Use of transmitochondrial cybrids to assign a complex I defect to the mitochondrial DNA-encoded NADH dehydrogenase subunit 6 gene mutation at nucleotide pair 14459 that causes Leber hereditary optic neuropathy and dystonia. Mol Cell Biol 1996;16:771–777.
13. MITOMAP: a human mitochondrial genome database. Atlanta, GA: Center for Molecular Medicine, Emory University. Available at: http://www.gen.emory.edu/mitomap.html. Accessed November 2001.
14. DiMauro S, Andreu AL. Mutations in mtDNA: are we scraping the bottom of the barrel? Brain Pathol 2000;10:431–441.
15. Wallace DC, Singh G, Lott MT, et al. Mitochondrial DNA mutation associated with Leber hereditary optic neuropathy. Science 1988;242:1427–1430.
16. Brown MD, Sun F, Wallace DC. Clustering of Caucasian Leber hereditary optic neuropathy patients containing the 11778 or 14484 mutations on an mtDNA lineage. Am J Hum Genet 1997;60:381–387.
17. Hofmann S, Jaksch M, Bezold R, et al. Population genetics and disease susceptibility: characterization of central European haplogroups by mtDNA mutations, correlation with D loop variants and association with disease. Hum Mol Genet 1997;6: 1835–1846.
18. Torroni A, Carelli V, Petrozzi M, et al. Detection of the mtDNA 14484 mutation on an African-specific haplotype: implications about its role in causing Leber hereditary optic neuropathy. Am J Hum Genet 1996;59:248–252.

# Brain Proteasomal Function in Sporadic Parkinson's Disease and Related Disorders

Yoshiaki Furukawa, MD,[1] Sophie Vigouroux, PhD,[2] Henry Wong, MSc,[1] Mark Guttman, MD,[3] Ali H. Rajput, MD,[4] Lee Ang, MD,[5] Marièle Briand, PhD,[2] Stephen J. Kish, PhD,[3] and Yves Briand, PhD[2]

**Because genetic defects relating to the ubiquitin–proteasome system were reported in familial parkinsonism, we evaluated proteasomal function in autopsied brains with sporadic Parkinson's disease. We found that proteasome peptidase activities in a fraction specific to the proteasome were preserved in five brain areas (including the striatum) of Parkinson's disease where neuronal loss is not observed. Striatal protein levels of two proteasome subunits were normal in Parkinson's disease but reduced mildly in disease controls (multiple system atrophy). Our brain data suggest that a systemic, global disturbance in the catalytic activity and degradation ability of the proteasome itself is unlikely to explain the cause of Parkinson's disease.**

Ann Neurol 2002;51:779–782

Findings of mutations in the genes encoding α-synuclein, ubiquitin carboxy-terminal hydrolase L1, and parkin in familial parkinsonism have suggested a role for the ubiquitin–proteasome system in the pathogenesis of sporadic Parkinson's disease (PD).[1–3] Misfolded, unassembled, or damaged cellular proteins are targeted for degradation by the ubiquitin–proteasome pathway.[4,5] This pathway involves two discrete processes: (1) covalent attachment of ubiquitin to the protein substrate and (2) degradation of the ubiquitin-conjugated protein by the 20/26S proteasome (the 20S proteasome is the catalytic core of the 26S proteasome).

Recently, McNaught and Jenner[6] reported moderately reduced peptidase activities of the proteasome in the substantia nigra of idiopathic PD and suggested that proteasomal inhibition may be a primary event arising from either gene defects or toxic substances. However, the determination of proteasome catalytic activities only in the substantia nigra (where dopaminergic neuronal loss exists) cannot exclude the possibility that the observed reduction is a secondary change associated with the neurodegenerative process. It is unknown whether possible failure of the degradation ability of the proteasome is restricted to brain regions of neuronal pathology or represents a systemic phenomenon in PD. To evaluate whether a global perturbation of brain proteasomal function is involved in the pathogenesis of sporadic PD, we measured proteasome peptidase activities with a fraction specific to the 20/26S proteasome and quantified protein levels of two proteasome subunits in autopsied striatum, cerebral cortices, and cerebellar cortex of PD patients and normal controls. In addition, the same brain areas in patients with multiple system atrophy (MSA) and progressive supranuclear palsy (PSP) were examined as disease controls with nigrostriatal dopaminergic degeneration.

## Patients and Methods

### *Patients and Controls*

Brain tissue was obtained from 28 patients with the clinical diagnosis of sporadic PD (9), MSA[7] (9), or PSP[8] (10). At autopsy, one half-brain was frozen for neurochemical analysis. A neuropathological examination of the other half-brain confirmed the diagnosis of PD with neuronal loss and Lewy bodies in the substantia nigra. Seven of the nine PD patients were treated with L-dopa up to the time of death. However, L-dopa has been reported to have no effect on proteasome peptidase activities[6] (but see Keller et al[9]). In the MSA brains, pathologic lesions in the nigrostriatal and olivopontocerebellar pathways[7,10] and heterogeneous high molecular weight α-synuclein-immunoreactive proteins (as reported by Dickson et al[11]) were observed (unpublished research). The PSP patients had a characteristic distribution of neurofibrillary tangles in the basal ganglia and brainstem.[8] For each neurochemical measurement, 10 to 12 neurologically and psychiatrically normal subjects, whose age and postmortem time were matched to the three patient groups, were used as controls.

### *Neurochemical Measurements*

Striatum (putamen and caudate) and cortices (frontal, occipital, and cerebellar) were used. Homogenized samples were centrifuged at 100,000*g* for 1 hour. The crude extract was subjected to chromatography on a Superose 6 column (Pharmacia, Piscataway, NJ). Two peaks (P1 and P2) were ob-

From the [1]Movement Disorders Research Laboratory, Centre for Addiction and Mental Health—Clarke Division, Toronto, Ontario, Canada; [2]Laboratoire de Biochimie Appliquée, Université Blaise Pascal, Clermont Ferrand, France; [3]Human Neurochemical Pathology Laboratory, Centre for Addiction and Mental Health—Clarke Division, Toronto, Ontario, Canada; [4]Division of Neurology, University of Saskatchewan, Saskatoon, Saskatchewan, Canada; and [5]Department of Pathology, University of Western Ontario, London, Ontario, Canada.

Received Nov 27, 2001, and in revised form Feb 6, 2002. Accepted for publication Feb 9, 2002.

Published online May 3, 2002, in Wiley InterScience (www.interscience.wiley.com). DOI: 10.1002/ana.10207

Address correspondence to Dr Furukawa, Movement Disorders Research Laboratory (R 211), Centre for Addiction and Mental Health—Clarke Division, 250 College Street, Toronto, Ontario, Canada M5T 1R8. E-mail: yoshiaki_furukawa@camh.net

 

served, and only P1 showed immunoreactivity of the 20/26S proteasome. However, both peaks had peptidase activities. Immunoprecipitation analysis with a proteasome specific antibody confirmed that catalytic activities of the proteasome were found only in P1. The additional centrifugation at 160,000*g* for 4.5 hours successfully separated the 20/26S proteasome (pellet) and an unknown protease (supernatant), and the pellet was used for proteasome activity and protein assays (vs simple tissue homogenates in the previous report[6]). Chymotrypsin-like (ChT-L), trypsin-like (T-L), and peptidyl glutamyl peptide hydrolase (PGPH) activities of the 20S proteasome were determined by the measurement of the fluorescence of 7-amido-4-methylcoumarin or 2-naphthylamide, which was generated from *N*-succinyl-LLVY-7-amido-4-methylcoumarin, LSTR-7-amido-4-methylcoumarin, and benzyloxycarbonyl-LLE-2-naphthylamide.[12] The proteasome inhibitor MG132[13] inhibited the ChT-L, T-L, and PGPH activities in the pellet by 99, 81, and 76%, respectively. The molecular weight of the unknown protease was estimated at approximately 105kDa (unpublished data), and the detailed characteristics of this protease are under investigation.

For Western blot analysis of two proteasome subunits in brain homogenates, the mouse monoclonal anti-iota (ι; 20S proteasome subunit α1; Cappel, Costa Mesa, CA) and anti-Tat binding protein 1 (Tbp1; 19S regulator subunit Rpt5; Affiniti Research, Mamhead, UK) antibodies were used as primary antibodies. Tbp1 was reported to interact with rat α-synuclein.[14] The peroxidase-linked antimouse immunoglobulin G antibody (Sigma, St. Louis, MO) was used as a secondary antibody. Immunoreactivities were visualized with chemiluminescence reagents and quantified by a computer-based imaging device (Fig 1). A one-way analysis of variance and a Student two-tailed *t* test were performed. Correlations were determined by Pearson product-moment correlation coefficients. The criterion of statistical significance was $p < 0.05$.

*Fig 1. Immunoreactivities of iota (ι) and Tat binding protein 1 (Tbp1) subunits of the proteasome in an autopsied brain of a normal control subject. Five concentrations (2.5–15μg/lane) of a tissue standard, consisting of a pool of human putamen, were loaded onto each gel to construct a standard curve (lanes S1–S5). The ι and Tbp1 immunoreactivities were detected as 29 and 53kDa bands in the putamen (P), caudate nucleus (CN), frontal cortex (F), occipital cortex (O), and cerebellar cortex (C). The amount of ι or Tbp1 protein was interpolated from the tissue standard curve run on the same gel.*

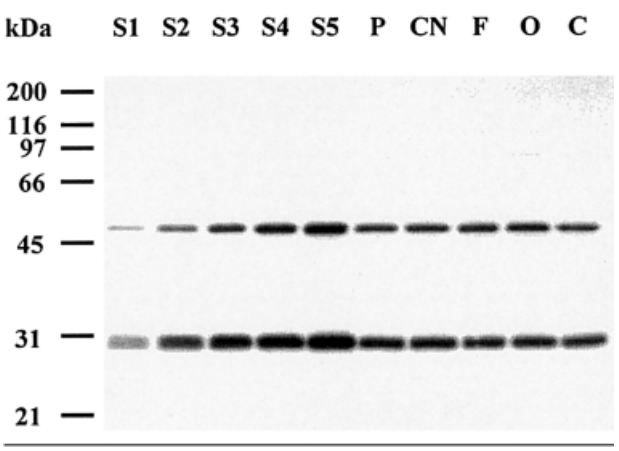


## Results

The ChT-L and T-L activities had a relatively homogeneous brain distribution in the controls (Table). There were no significant decreases in these activities in the PD, MSA, and PSP patients compared with those in the controls. Regression analysis showed a significant positive correlation between ChT-L and T-L activity levels in all of the five brain regions ($r = 0.57–0.75$, $p < 0.001$). In the controls, ι and Tbp1 protein concentrations in the cerebellar cortex were lower than those in the four other brain areas. Brain protein levels of ι and Tbp1 were preserved in the PD patients with the exception of a mild loss of Tbp1 in the occipital cortex, where a slight reduction of ι was observed in the MSA and PSP groups. Both ι and Tbp1 protein levels in the striatum were reduced by 14 to 26% in the MSA group in comparison with the control means. In the striatum of the PSP patients, protein concentrations of Tbp1 were normal, but ι protein levels were mildly reduced in the caudate nucleus. An additional measurement of PGPH activity in the caudate nucleus, however, showed that mean levels of this proteasome peptidase activity in the PD (mean, 8.66nmol/mg of protein/30min; SE, 1.36), MSA (mean, 8.50nmol/mg of protein/30min; SE, 1.43), and PSP (mean, 5.75nmol/mg of protein/30min; SE, 1.43) groups were also not significantly different from that in the control group (mean, 5.34nmol/mg of protein/30min; SE, 1.21). The levels of PGPH activity were positively correlated with those of ChT-L and T-L activities ($r = 0.79$ and 0.54, $p < 0.001$).

## Discussion

The major finding of our study is that proteasome peptidase activities in a brain fraction specific to the 20/26S proteasome were preserved in the striatum and cortices of PD, MSA, and PSP.

The 20S proteasome, a multicatalytic proteinase, combines with the 19S regulator complex to form the 26S proteasome, which is responsible for ubiquitin-ATP-dependent proteolysis.[4,5] This 20S proteasome also can degrade oxidatively modified proteins in an ubiquitin-ATP-independent manner.[15] The ChT-L, T-L, and PGPH activities of the 20S proteasome preferentially cleave bonds after hydrophobic, basic, and acidic amino acid residues. Under our experimental conditions in which other proteases (including the 105kDa protease; see the Patients and Methods section) were eliminated, the fluorogenic substrates used to measure the three peptidase activities were specific for the proteasome, and the ability of the proteasome to cleave the peptide substrates was not reduced in the

*Table. Chymotrypsin-like and Trypsin-like Activities and Iota and Tat Binding Protein 1 Protein Levels in the Brain of Parkinson's Disease, Multiple System Atrophy, and Progressive Supranuclear Palsy Patients and of Normal Controls*

| Variable | No. of Patients[a] | Putamen | Caudate Nucleus | Frontal Cortex | Occipital Cortex | Cerebellar Cortex |
|---|---|---|---|---|---|---|
| ChT-L activity | | | | | | |
| Controls | 10 | 7.61 ± 1.70 | 7.86 ± 1.35 | 9.11 ± 1.88 | 8.22 ± 1.58 | 7.71 ± 1.47 |
| PD | 8 | 8.70 ± 1.08 | 10.67 ± 1.29 | 10.41 ± 1.28 | 8.05 ± 0.98 | 10.20 ± 1.44 |
| MSA | 8 | 9.06 ± 1.59 | 11.31 ± 1.48 | 11.00 ± 1.66 | 10.33 ± 1.37 | 10.25 ± 1.45 |
| PSP | 10 | 6.74 ± 1.36 | 8.21 ± 1.94 | 7.26 ± 1.96 | 4.74 ± 1.11 | 5.42 ± 1.19 |
| ANOVA | | NS | NS | NS | $p < 0.05$ | NS |
| T-L activity | | | | | | |
| Controls | 10 | 2.88 ± 0.35 | 2.55 ± 0.25 | 2.78 ± 0.23 | 2.49 ± 0.29 | 2.48 ± 0.26 |
| PD | 8 | 3.02 ± 0.29 | 3.28 ± 0.23 | 3.32 ± 0.44 | 2.77 ± 0.18 | 3.35 ± 0.32[b] |
| MSA | 8 | 2.91 ± 0.29 | 3.23 ± 0.22 | 2.96 ± 0.20 | 2.69 ± 0.30 | 3.02 ± 0.27 |
| PSP | 10 | 2.82 ± 0.34 | 3.10 ± 0.62 | 2.60 ± 0.37 | 2.13 ± 0.25 | 2.12 ± 0.23 |
| ANOVA | | NS | NS | NS | NS | $p < 0.05$ |
| Iota protein | | | | | | |
| Controls | 12 | 11.42 ± 0.30 | 12.96 ± 0.47 | 10.06 ± 0.36 | 11.61 ± 0.31 | 8.54 ± 0.36 |
| PD | 9 | 11.75 ± 0.30 | 12.07 ± 0.57 | 9.80 ± 0.40 | 11.13 ± 0.66 | 10.11 ± 0.24[c] |
| MSA | 9[d] | 8.93 ± 0.19[e] | 9.94 ± 0.43[e] | 9.43 ± 0.27 | 10.03 ± 0.42[f] | 10.29 ± 0.31[c] |
| PSP | 10[g] | 11.50 ± 0.62 | 10.42 ± 0.45[e] | 10.03 ± 0.22 | 9.95 ± 0.38[c] | 10.09 ± 0.67[b] |
| ANOVA | | $p < 0.001$ | $p < 0.001$ | NS | $p < 0.05$ | $p < 0.05$ |
| Tbp1 protein | | | | | | |
| Controls | 12 | 12.96 ± 0.43 | 14.28 ± 0.46 | 14.97 ± 0.56 | 16.49 ± 0.65 | 12.56 ± 0.81 |
| PD | 9 | 12.62 ± 0.76 | 12.96 ± 0.44 | 14.67 ± 0.77 | 13.41 ± 0.66[c] | 13.48 ± 0.50 |
| MSA | 9[d] | 9.55 ± 1.07[c] | 12.28 ± 0.59[b] | 15.92 ± 0.63 | 14.65 ± 0.63 | 11.29 ± 0.74 |
| PSP | 10[g] | 13.76 ± 0.68 | 13.28 ± 0.41 | 14.65 ± 0.38 | 15.03 ± 0.36 | 13.15 ± 0.51 |
| ANOVA | | $p < 0.005$ | $p < 0.05$ | NS | $p < 0.01$ | NS |

ChT-L and T-L activity assays were triplicated and values are expressed as mean ± SE (nmol/mg protein/30 min). Iota and Tbp1 protein measurements were duplicated, and values are expressed as mean ± SE (μg tissue standard/10μg protein). There were no significant differences among mean values of age and postmortem time of 12 controls (71 ± 3 years, 13 ± 2 hours), nine PD patients (74 ± 2, 14 ± 2), 9 MSA patients (68 ± 1, 13 ± 2), and 10 PSP patients (73 ± 3, 13 ± 1) (one-way ANOVA).

[a]ChT-L and T-L activities were determined in 10 of the 12 controls, eight of the nine PD patients, and eight of the nine MSA patients.
[b]$p < 0.05$. All $p$ values are for the differences from the controls (Student's two-tailed $t$ test).
[c]$p < 0.005$.
[d]Putamen and cerebellar cortex tissues were available in eight of the nine MSA patients.
[e]$p < 0.001$.
[f]$p < 0.01$.
[g]Cerebellar cortex tissue was available in 9 of the 10 PSP patients.

ChT-L = chymotrypsin-like; T-L = trypsin-like; Tbp1 = Tat binding protein 1; PD = Parkinson's disease; MSA = multiple system atrophy; PSP = progressive supranuclear palsy; NS = not significant.

five brain areas of PD, MSA, and PSP. Several lines of evidence have shown relationships between mutations identified in familial parkinsonism and the ubiquitin–proteasome system: (1) mutant α-synuclein was degraded less efficiently than the wild type by this system[1] (but see Ancolio et al[16] and Paxinou et al[17]), (2) a mutation in the ubiquitin carboxy-terminal hydrolase L1 gene resulted in low activity of this deubiquitinating enzyme,[2] and (3) parkin was found to be a ubiquitin ligase.[3] However, none of these findings indicate dysfunction of the 20S proteasome itself.

Both ι and Tbp1 protein concentrations were reduced only in the striatum of MSA, whereas slight changes in protein levels of one of the subunits were observed in some brain regions of the diseases. The cause of this mild but significant striatal protein loss of the subunits in MSA is unknown. Because there are many α-synuclein-positive glial cytoplasmic inclusions in the striatum of MSA, the proteasome subunits could be affected by proteins (including α-synuclein) modified by oxidation and nitration.[11,17] Nevertheless, striatal levels of all of the three peptidase activities of the 20S proteasome were well preserved or showed a tendency to increase in the MSA patients (Fig 2), suggesting that there may be a compensatory mechanism or upregulation. Alternatively, the decreased subunit proteins and increased catalytic activities of the proteasome in MSA might be the result of striatal neuronal loss (should these neurons be preferentially enriched in the proteasome) and gliosis. Proteasome immunoreactivity is present in both neuronal and glial cells throughout the rat brain and is predominantly localized in the nucleus.[18] It has been suggested that mitotic cells (glia) may

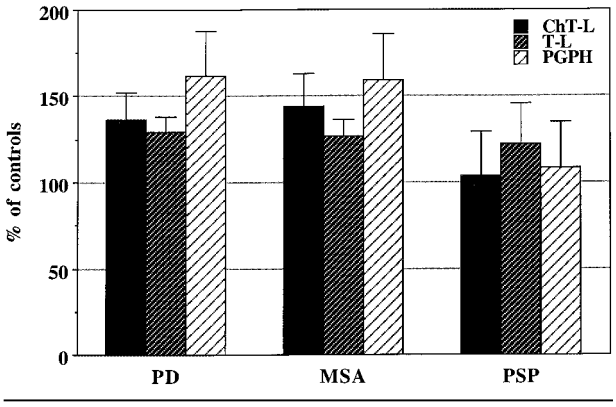


*Fig 2. Mean levels of chymotrypsin-like (ChT-L), trypsin-like (T-L), and peptidyl glutamyl peptide hydrolase (PGPH) activities of the proteasome in the caudate nucleus of patients with Parkinson's disease (PD), multiple system atrophy (MSA), and progressive supranuclear palsy (PSP) expressed as percentages of the control means (plus or minus the standard error). There were no significant differences among mean values of age and postmortem time for 10 controls (age: mean, 69 years; SE, 3; time: mean, 13 hours; SE, 2), eight PD patients (age: mean, 75 years; SE, 2; time: mean, 14 hours; SE, 2), eight MSA patients (age: mean, 67 years; SE, 1; time: mean, 13 hours; SE, 2), and 10 PSP patients (age: mean, 73 years; SE, 3; time: mean, 13 hours; SE, 1; one-way analysis of variance).*

have higher activities of the proteasome than postmitotic cells (neurons).[19]

The failure of proteasomal function caused by defects in the genes encoding its subunits has been suggested in idiopathic PD.[6] However, this appears unlikely because the peptidase activities in the morphologically unaffected brain regions of PD were preserved in our study, indicating that there is no systemic dysfunction of the proteasome in this disorder. Protein aggregation and severe oxidative injury can inhibit the ubiquitin–proteasome pathway.[15,20] The reported reduction of proteasome activities in the substantia nigra of PD[6] might be explained by a secondary phenomenon associated with degeneration of nigrostriatal dopaminergic neurons or by neuronal loss itself.

In conclusion, our data suggest that brain proteasomal function (catalytic activity and degradation ability) itself is globally preserved in sporadic PD as well as MSA and PSP.

This study was supported in part by the William S. Storey and Al Silverberg PSP Funds, the Friedman MSA Fund, and the Centre for Addiction and Mental Health Foundation.

## References

1. Bennett MC, Bishop JF, Leng Y, et al. Degradation of α-synuclein by proteasome. J Biol Chem 1999;274: 33855–33858.
2. Leroy E, Boyer R, Auburger G, et al. The ubiquitin pathway in Parkinson's disease. Nature 1998;395:451–452.
3. Shimura H, Schlossmacher MG, Hattori N, et al. Ubiquitination of a new form of α-synuclein by parkin from human brain: implications for Parkinson's disease. Science 2001;293: 263–269.
4. Schwartz AL, Ciechanover A. The ubiquitin–proteasome pathway and pathogenesis of human diseases. Annu Rev Med 1999; 50:57–74.
5. Orlowski M, Wilk S. Catalytic activities of the 20 S proteasome, a multicatalytic proteinase complex. Arch Biochem Biophys 2000;383:1–16.
6. McNaught KSP, Jenner P. Proteasomal function is impaired in substantia nigra in Parkinson's disease. Neurosci Lett 2001;297: 191–194.
7. Gilman S, Low PA, Quinn N, et al. Consensus statement on the diagnosis of multiple system atrophy. J Neurol Sci 1999; 163:94–98.
8. Litvan I, Agid Y, Calne D, et al. Clinical research criteria for the diagnosis of progressive supranuclear palsy (Steele-Richardson-Olszewski syndrome): report of the NINDS-SPSP international workshop. Neurology 1996;47:1–9.
9. Keller JN, Huang FF, Dimayuga ER, Maragos WF. Dopamine induces proteasome inhibition in neural PC12 cell line. Free Radic Biol Med 2000;29:1037–1042.
10. Wenning GK, Ben-Shlomo Y, Magalhàes M, et al. Clinicopathological study of 35 cases of multiple system atrophy. J Neurol Neurosurg Psychiatry 1995;58:160–166.
11. Dickson DW, Liu W-K, Hardy J, et al. Widespread alterations of α-synuclein in multiple system atrophy. Am J Pathol 1999; 155:1241–1251.
12. Farout L, Lamare MC, Cardozo C, et al. Distribution of proteasomes and of the five proteolytic activities in rat tissues. Arch Biochem Biophys 2000;374:207–212.
13. Lee DH, Goldberg AL. Selective inhibitors of the proteasome-dependent and vacuolar pathways of protein degradation in *Saccharomyces cerevisiae*. J Biol Chem 1996;271:27280–27284.
14. Ghee M, Fournier A, Mallet J. Rat α-synuclein interacts with Tat binding protein 1, a component of the 26S proteasomal complex. J Neurochem 2000;75:2221–2224.
15. Davies KJA. Degradation of oxidized proteins by the 20S proteasome. Biochimie 2001;83:301–310.
16. Ancolio K, Alves da Costa C, Uéda K, Checler F. α-Synuclein and the Parkinson's disease-related mutant Ala53Thr-α-synuclein do not undergo proteasomal degradation in HEK293 and neuronal cells. Neurosci Lett 2000;285:79–82.
17. Paxinou E, Chen Q, Weisse M, et al. Induction of α-synuclein aggregation by intracellular nitrative insult. J Neurosci 2001;21: 8053–8061.
18. Mengual E, Arizti P, Rodrigo J, et al. Immunohistochemical distribution and electron microscopic subcellular localization of the proteasome in the rat CNS. J Neurosci 1996;16: 6331–6341.
19. Ding Q, Keller JN. Proteasomes and proteasome inhibition in the central nervous system. Free Radic Biol Med 2001;31: 574–584.
20. Bence NF, Sampat RM, Kopito RR. Impairment of the ubiquitin–proteasome system by protein aggregation. Science 2001; 292:1552–1555.

# Increased Expression of the Amyloid Precursor β-Secretase in Alzheimer's Disease

R. M. Damian Holsinger, MSc,[1]
Catriona A. McLean, MD,[1] Konrad Beyreuther, PhD,[2]
Colin L. Masters, MD,[1] and Geneviève Evin, PhD[1]

**β-Secretase cleavage represents the first step in the generation of Aβ polypeptides and initiates the amyloid cascade that leads to neurodegeneration in Alzheimer's disease. By comparative Western blot analysis, we show a 2.7-fold increase in protein expression of the β-secretase enzyme BACE in the brain cortex of Alzheimer's disease patients as compared to age-matched controls. Similarly, we found the levels of the amyloid precursor protein C-terminal fragment produced by β-secretase to be increased by nearly twofold in Alzheimer's disease cortex.**

Ann Neurol 2002;51:783–786

Aβ amyloid deposition is the pathological feature of Alzheimer's disease (AD), and cytotoxic Aβ oligomers are considered to be responsible for neuronal degeneration.[1] Aβ is derived from a type I integral membrane amyloid precursor protein (APP), by two consecutive proteolytic cleavages caused by β- and γ-secretases (reviewed in Selkoe[1] and Vassar and Citron[2]). These proteases represent the prime targets for drug design. A β-secretase gene that encodes the novel, transmembrane aspartyl protease BACE has been unraveled by several groups.[3–7] Gene ablation experiments have demonstrated that BACE is required for Aβ formation, providing definitive evidence that it is β-secretase.[8–10] We have studied the expression of BACE in human brain by Western blotting and by quantitative, competitive reverse transcription-polymerase chain reaction (RT-PCR). We report a significant 2.7-fold increase in BACE protein expression in sporadic AD brain as compared to controls.

From the [1]Department of Pathology, The University of Melbourne and the Mental Health Research Institute, Parkville, Victoria, Australia; and [2]Center for Molecular Biology, ZMBH, University of Heidelberg, Heidelberg, Germany.

Received Aug 21, 2001, and in revised form Feb 11, 2002. Accepted for publication Feb 11, 2002.

Published online May 21, 2002, in Wiley InterScience (www.interscience.wiley.com). DOI: 10.1002/ana.10208

Address correspondence to Dr Evin, Department of Pathology, The University of Melbourne, Parkville, Victoria 3010, Australia. E-mail: gmevin@unimelb.edu.au

## Patients and Methods

### *Brain Sample Preparation*

Brain tissue samples were obtained from the NH&MRC Tissue Resource Centre (Melbourne, Australia) and from the Institute for Brain Aging and Dementia Tissue Repository (Irvine, CA). The control group consisted of 10 normal patients aged 53 to 86 (mean age 74 ± 3) and 8 patients with neurological diseases other than AD (2 Parkinson's disease, 3 frontotemporal dementia, and 3 Huntington's disease) aged 43 to 84 (mean age 69 ± 4). The sporadic AD group consisted of 16 patients aged 65 to 85 (mean age 78 ± 2) with no history of familial AD and no identified mutations. Frontal lobe tissue (≈100mg) was homogenized in TRIzol (Life Technologies, Melbourne, Australia). RNA and protein was extracted following the manufacturer's recommendations. The protein pellet was dissolved in 1% sodium dodecyl sulfate. Protein concentration was determined using the bicinchoninic acid reagent (Pierce, Rockford, IL).

### *Cloning of BACE*

Full-length BACE was cloned by RT-PCR from total RNA extracted from human cortical brain tissue. This was sequenced, subcloned into the pcDNA3.1+ expression vector (Invitrogen, Groningen, The Netherlands), and overexpressed in CHO cells.

### *Western Blotting and Quantitation*

Rabbit polyclonal antiserum 00/6 was raised to human BACE [485–501]. Monoclonal anti-β-tubulin antibody was purchased from Sigma (St. Louis, MO). Antibody to α-synuclein [116–131][11] was obtained from J. Culvenor, and APP [645–694] antibody 369 was a gift from S. Gandy[12] (New York University, Orangeburg, NY). Horseradish peroxidase conjugated secondary antibodies were from Amersham-Pharmacia Biotech (Castle Hill, Australia). Aβ monoclonal antibody WO2 has been previously described.[13] Twenty-five micrograms of protein were separated by SDS-PAGE on 8.5% acrylamide gels under reducing conditions and transferred to nitrocellulose. The membranes were blocked with 5% skimmed-milk powder (w/v) and 1% (w/v) bovine serum albumin in Tris-buffered saline (10mM Tris/HCl, pH 8.0, 150mM NaCl) containing 0.5% Tween-20, and probed with primary (00/6 at 1:1500 dilution in blocking buffer) and secondary antibody followed by enhanced-chemiluminescence (ECL) detection (Amersham). The films were scanned and the bands quantitated by densitometry using the NIH Image 1.60 software. Data were normalized to the levels of constitutively expressed neuronal markers β-tubulin and α-synuclein. Statistical analysis was performed using the SPSS software package for Windows (SPSS, Chicago, IL). Data were expressed as mean ± standard error of the mean. A $p = 0.05$ level of statistical significance was used in all tests.

### *Quantitative Reverse Transcription-Polymerase Chain Reaction*

The method we described preivously[14] was modified as follows. A deletion standard was constructed by deleting a 289bp *Avr* II-*Bgl* II restriction enzyme fragment from the BACE mouse gene (selected for its homology to human

 

BACE sequence) and was subcloned into a pGEM-T Easy vector (Promega Biotech, Annandale, Australia). This was transcribed using the T7 promoter (Promega) and a MEGAscript Kit (Ambion, Austin, TX). The primers used for BACE transcript analysis amplified a 408bp human BACE fragment and a 119bp BACE deletion standard. Amplification of endogenous β-actin transcripts was as previously reported.[14] cDNA was synthesized as previously described.[14] Each tube contained 1μg human frontal cortical total RNA and one dilution (0.5–5pg) of BACE deletion standard RNA. cDNA amplification was carried out as follows: denaturation at 94°C for 2 minutes, followed by 35 cycles of denaturation at 94°C for 15 seconds, primer annealing at 69°C for 30 seconds, and extension at 72°C for 45 seconds. A final extension was carried out at 72°C for 7 minutes, ending with a 4°C hold cycle.

**Results and Discussion**

To analyze the expression of BACE in human brain, we developed comparative Western blotting and quantitative, competitive RT-PCR. Initially, we cloned the BACE gene by RT-PCR from total RNA of human cortical tissue from a control patient. Sequencing showed a one base-pair, C→T polymorphism at position 967 (numbering as in Vassar and colleagues[3]). This sequence was subcloned into the pcDNA3.1+ vector, transfected into CHO cells, and used to confirm the specificity of polyclonal antibody 00/6. In immunoblotting experiments, this antibody detected a 70kDa signal in lysates from BACE transfected cells and a 70-72kDa doublet in human brain homogenates. This result is consistent with the molecular mass of BACE and with previous reports.[3,4]

Comparative analysis of brain samples from normal control (Fig 1a, lanes 1–4) and sporadic AD patients (see Fig 1a, lanes 5–10) suggested an elevated BACE expression in AD. To assess this finding, a larger series of samples were studied including sporadic AD, age-matched normal controls, and neurological diseases other than AD (termed neurological controls). All AD samples were pathologically diagnosed in accordance with CERAD (Consortium to Establish a Registry for Alzheimer's Disease) criteria.[15] For a comparative analysis of BACE in AD and controls, the 70-72kDa doublet was quantitated by image densitometry. The data were normalized relative to the Western blot signals of β-tubulin (see Fig 1b) and of the neuronal protein α-synuclein. Analysis of variance showed a statistically significant, 2.7-fold increase in the BACE/β-tubulin signals in AD ($p = 0.002$) as compared to control samples (see Fig 1c). The intensity of β-tubulin signal did not differ significantly between the normal control and the AD groups ($p = 0.44$, Student's $t$ test), or between the neurological control and the AD groups ($p = 0.10$). Similarly, the ratio of BACE/α-synuclein signal was increased by 2.5-fold in AD (not shown). Regression analysis did not reveal any trend between the age of the patients and the intensity of the BACE signal, either in the control ($r = 0.35$; $p = 0.31$) or in the AD group ($r = 0.21$; $p = 0.42$). A similar quantitative analysis was applied to β-CTF, the C-terminal fragment of APP produced by β-secretase cleavage. This fragment was detected as a 14kDa protein immunoreactive with antibodies 369 (directed to APP cyto-

*Fig 1. BACE immunoreactivity is increased in Alzheimer's disease brain. Cortical protein extracts were resolved by polyacrylamide gel electrophoresis, transferred to nitrocellulose membranes and the blots probed with antibodies to (a) BACE (00/6) or (b) β-tubulin. C = control; AD = sporadic AD. (c) BACE and β-tubulin signals were quantitated by image densitometry, and ratios of BACE/β-tubulin signals were statistically analyzed. The control group consisted of 10 normal (mean age 74 ± 3) and 8 neurological control patients (2 with Parkinson's disease, 3 with frontotemporal dementia, and 3 with Huntington's disease; mean age 69 ± 4). The Alzheimer's disease group consisted of 16 patients (mean age 78 ± 2).*

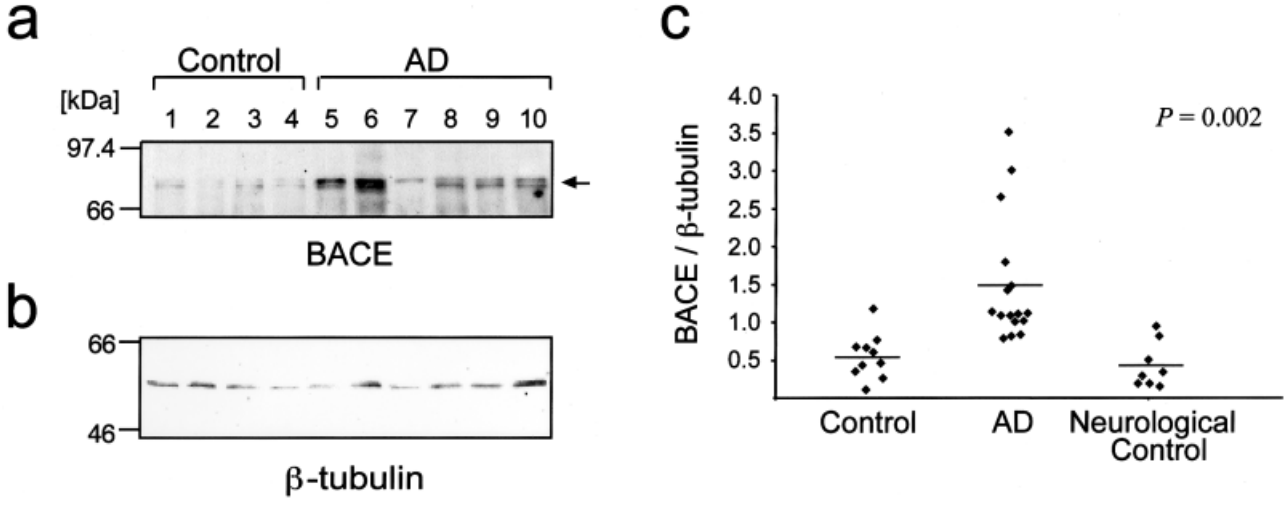

plasmic domain) and with WO2 (directed to Aβ N-terminus) as previously described.[16] A statistically significant 1.8-fold increase in β-CTF/β-tubulin signals ($p = 0.04$) was observed in AD compared to controls (Fig 2). This data would support an increase in β-secretase activity in AD.

To establish whether increase of BACE protein expression in AD brain resulted from an alteration in message expression, we quantitated BACE mRNA levels in the cortical samples using competitive RT-PCR.[14] An average of 0.5pg to 1pg of BACE mRNA per microgram of human frontal cortex total RNA was detected, and this value did not differ between control and AD samples (Fig 3). This result corroborates a report by others showing that mRNA for APP, BACE, and the putative α-secretase, ADAM10, are expressed at similar levels in cortical brain tissue of AD and control patients.[17] It is also consistent with a study based on a population of 581 patients, including 239 AD, that demonstrates the absence of a genetic linkage between the BACE locus and an increased incidence of AD.[18] Taken together, our findings suggest that the increased BACE immunoreactivity in AD brain would reflect an alteration in protein metabolism and not in message expression.

Familial AD has been associated with mutations in the presenilin genes (PS1 and PS2), or in the APP gene, at or near the β- and γ-secretase cleavage sites. One of the APP mutations (codons 670/671; referred to as the Swedish mutation) has been reported to affect β-secretase cleavage by providing a better substrate for the enzyme. This mutation causes a six- to eightfold overproduction of Aβ[19] and highlights the potential importance of β-secretase in AD pathogenesis. Here we have shown a significant increase in BACE immunoreactivity in sporadic AD and concomitant increase in the levels of APP β-CTF, the direct precursor of Aβ. Whereas the widespread expression of BACE gene in neuronal and peripheral tissues[3,4,6] may suggest it is a ubiquitous protease and could potentially cleave substrates other than APP, the results of gene ablation experiments have proved that BACE knockout mice are viable and apparently normal.[8,9] Therefore, a rational approach to reducing Aβ production based on BACE inhibition would represent a promising therapeutic strategy for AD. The mechanism leading to the increased levels of BACE protein in AD brain is currently under investigation as it may constitute a determining factor in the pathogenesis of sporadic AD.

*Fig 2. Quantitative analysis of β-CTF, the C-terminal fragment of amyloid precursor protein produced by β-secretase cleavage, shows an increase in Alzheimer's disease. Cortical protein extracts were analyzed by Western blotting with antibody 369 (directed to amyloid precursor protein cytoplasmic domain). β-CTF was detected as a 14kDa band. This signal was quantitated by image densitometry and the data were normalized to β-tubulin before statistical analysis. A significant 1.8-fold increase was observed in Alzheimer's disease (n = 9) as compared to controls (n = 8).*

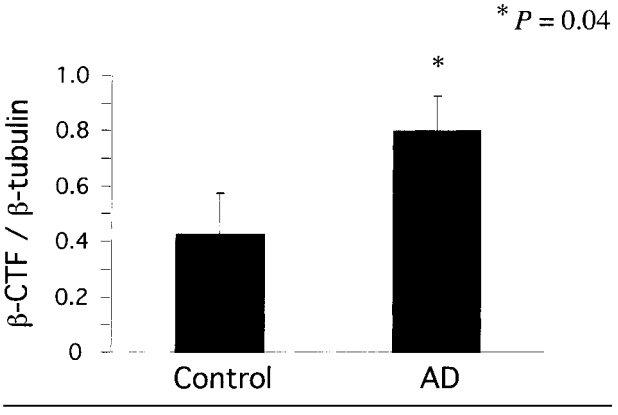


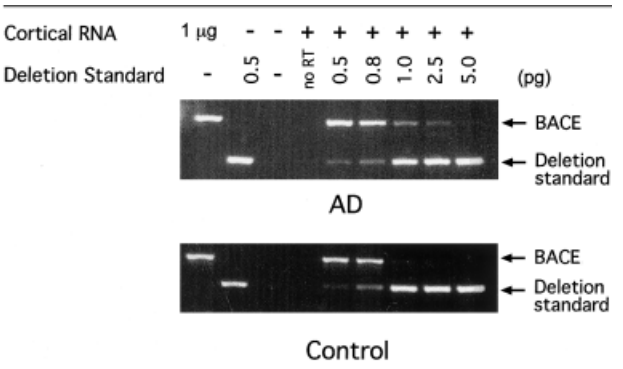


*Fig 3. mRNA expression of BACE is similar in Alzheimer's disease and control brains. For quantitative, competitive reverse transcription-polymerase chain reaction (RT-PCR)[14] of BACE mRNA deletion standard was constructed by deleting a 289bp fragment from the BACE mouse gene in a region homologous to human BACE by restriction enzyme digestion. The primers used for BACE transcript analysis amplified a 408bp human BACE fragment and a 119bp BACE deletion standard. Each tube contained 1μg of human frontal cortex total RNA and one dilution (0.5–5pg) of deletion standard. Polymerase chain reaction was performed on the entire reverse transcribed cDNA sample and analyzed as reported previously.[14]*

This work was supported in part by the NH&MRC (114150, G.E., C.L.M.). K.B. is supported by the Deutsche Forschungsgemeinschaft and the Bundesministerium für Forschung und Technologie.

We thank A. F. Hill, D. Hoke, J. G. Culvenor, and A. Weidemann for critical reading of the manuscript.

## References

1. Selkoe DJ. Translating cell biology into therapeutic advances in Alzheimer's disease. Nature 1999;399:23–31.
2. Vassar R, Citron M. Aβ-generating enzymes: recent advances in β- and γ-secretase research. Neuron 2000;27:419–422.

3. Vassar R, Bennett BD, Babu-Khan S, et al. β-secretase cleavage of Alzheimer's amyloid precursor protein by the transmembrane aspartic protease BACE. Science 1999;286:735–741.
4. Sinha S, Anderson JP, Barbour R, et al. Purification and cloning of amyloid precursor protein β-secretase from human brain. Nature 1999;402:537–540.
5. Yan R, Bienkowski MJ, Shuck ME, et al. Membrane-anchored aspartyl protease with Alzheimer's disease β-secretase activity. Nature 1999;40:533–537.
6. Hussain I, Powell D, Howlett DR, et al. Identification of a novel aspartic protease (Asp2) as β-secretase. Mol Cell Neurosci 1999;14:419–427.
7. Lin X, Koelsch G, Wu S, et al. Human aspartic protease memapsin 2 cleaves the beta-secretase site of beta-amyloid precursor protein. Proc Natl Acad Sci U S A 1999;97:1456–1460.
8. Luo Y, Bolon B, Kahn S, et al. Mice deficient in BACE1, the Alzheimer's β-secretase, have normal phenotype and abolished β-amyloid generation. Nat Neurosci 2001;4:231–232.
9. Cai H, Wang Y, McCarthy D, et al. BACE1 is the major β-secretase for generation of Aβ peptides by neurons. Nat Neurosci 2001;4:233–234.
10. Roberds SL, Anderson J, Basi G, et al. BACE knockout mice are healthy despite lacking the primary β-secretase activity in brain: implications for Alzheimer's disease therapeutics. Hum Mol Genet 2001;10:1317–1324.
11. Culvenor JG, McLean CA, Cutt S, et al. Non-Aβ component of Alzheimer's disease amyloid (NAC) revisited. Am J Pathol 1999;155:1173–1181.
12. Buxbaum JD, Gandy SE, Cicchetti P, et al. processing of Alzheimer's β/A4 amyloid precursor protein: modulation by agents that regulate protein phosphorylation. Proc Natl Acad Sci U S A 1990;87:6003–6006.
13. Ida N, Hartmann T, Pantel J, et al. Analysis of heterogeneous A4 peptides in human cerebrospinal fluid and blood by a newly developed sensitive Western blot assay. J Biol Chem 1996;271: 22908–22914.
14. Holsinger RMD, Schnarr J, Henry P, et al. Quantitation of BDNF mRNA in human parietal cortex by competitive reverse transcription-polymerase chain reaction: decreased levels in Alzheimer's disease. Mol Brain Res 2000;76:347–354.
15. Mirra SS, Heyman A, McKeel D, et al. The consortium to establish a registry for Alzheimer's disease (CERAD). Part II. Standardization of the neuropathologic assessment of Alzheimer's disease. Neurology 1991;41:479–486.
16. Evin G, Cappai R, Li QX, et al. Candidate gamma-secretases in the generation of the carboxyl terminus of the Alzheimer's disease beta A4 amyloid: possible involvement of cathepsin D. Biochemistry 1995;34:14185–14192.
17. Marcinkiewicz M, Seidah NG. Coordinated expression of beta-amyloid precursor protein and the putative beta-secretase BACE and alpha-secretase ADAM10 in mouse and human brain. J Neurochem 2000;75:2133–2143.
18. Murphy T, Yip A, Brayne C, et al. The BACE gene: genomic structure and candidate gene study in late-onset Alzheimer's disease. Neuroreport 2001;12:631–634.
19. Citron M, Oltersdorf T, Haass C, et al. Mutation of the beta-amyloid precursor protein in familial Alzheimer's disease increases beat-protein production. Nature 1992;360:672–674.

# High Headache Prevalence among Women with Hemochromatosis: The Nord-Trøndelag Health Study

Knut Hagen, MD,[1] Lars Jacob Stovner, PhD,[1] Arne Åsberg, MD,[2] Ketil Thorstensen, PhD,[2] Kristian S. Bjerve, PhD,[2] and Kristian Hveem, PhD[3]

**In this large cross-sectional population-based study, 51,272 persons responded to a headache questionnaire and were screened for hemochromatosis. Phenotypic hemochromatosis and the C282Y/C282Y genotype were both associated with an 80% increase in headache prevalence evident only among women. The reason for this association is unclear, but one may speculate that iron overload alters the threshold for triggering a headache by disturbing neuronal function.**

Ann Neurol 2002;51:786–789

Hemochromatosis is an autosomal recessive disease that causes an inappropriately high absorption of iron, leading to progressive accumulation of iron in the liver, pancreas, pituitary gland, and other organs.[1] Iron is necessary for normal neuronal function, but the iron homeostasis must be stringently regulated to avoid iron-induced oxidative injury, and iron overload may induce neuronal damage in the brain.[2]

Two mutations in the hemochromatosis gene (HFE gene) on chromosomal locus 6p21 have been identified, and in Norway 88% of individuals with newly diagnosed hemochromatosis were homozygous for the C282Y mutation (tyrosine replacing cysteine at amino acid 282), whereas the H63D mutation (aspartate replacing histidine at amino acid 63) was present in 7% of the cases.[3]

During the past year, we have seen several headache

From the [1]Department of Clinical Neuroscience, Section of Neurology, Norwegian University of Science and Technology, Trondheim, Norway; [2]Department of Clinical Chemistry, Trondheim University Hospital, Trondheim, Norway; and [3]Innherred Hospital, Levanger, Norway.

Received Nov 26, 2001, and in revised form Feb 11, 2002. Accepted for publication Feb 11, 2002.

Published online May 3, 2002, in Wiley InterScience (www.interscience.wiley.com). DOI: 10.1002/ana.10209

Address correspondence to Dr Hagen, Department of Clinical Neuroscience, Faculty of Medicine, Norwegian University of Science and Technology, 7006 Trondheim, Norway.
E-mail: knut.hagen@medisin.ntnu.no

 

patients with hemochromatosis, but there are no observational studies on the possible association between the two disorders. With data from a large-scale health survey, the aim of this study was to examine a possible association between headache and phenotypic hemochromatosis and between headache and HFE genotype.

## Subjects and Methods

Between 1995 and 1997, all inhabitants 20 years of age or older in Nord-Trøndelag County in Norway were invited to enter a health survey program (the HUNT study) encompassing about 40 subprojects. Two of these projects were a screening for hemochromatosis and a questionnaire-based study of headaches (Head-HUNT). Of 92,566 persons invited, a total of 51,282 subjects (55%) both responded to the headache questionnaire and participated in the screening for hemochromatosis.

### *Hemochromatosis: Screening and Diagnosis*

Details of the screening and diagnosis of phenotypic and genotypic hemochromatosis have been reported elsewhere.[3] Briefly, if the serum transferrin saturation, which was used for screening, was more than 50% for women and 55% for men, the test was considered positive and repeated after an overnight fast. If the second test was also positive, ferritin in serum was analyzed (reference limits: 110μg/L for women and 200μg/L for men). Subjects were also assessed for other factors causing secondary iron overload, including diet, blood transfusions, alcohol, and liver and hematological diseases.[3] Individuals with high serum transferrin saturation in two separate blood samples and serum ferritin concentrations above the reference limit and no other conditions that could explain the high serum ferritin were considered to have phenotypic hemochromatosis.

All subjects with high serum transferrin saturation in two tests were offered genotyping.[3] A total of 91% accepted, and genomic DNA was isolated from anticoagulated venous blood and amplified by polymerase chain reaction with primers as described previously.[3]

The prevalence of phenotypic hemochromatosis was 0.34% in women and 0.68% in men, and the prevalence of the C282Y/C282Y mutation was at least 0.68%.[3]

### *Headache Diagnosis*

HUNT also included 13 headache questions,[4] and individuals who answered "yes" to the question "Have you suffered from headache during the last 12 months?" were classified as "headache sufferers." According to data from the subsequent 12 headache questions, they were classified into two groups: migrainous and nonmigrainous. Persons were diagnosed as migraine sufferers if they self-reported migraine headaches or fulfilled the following three criteria: (1) headache attacks lasted from 4 to 72 hours (72 hours or less for those who reported frequent visual disturbances before the attacks); (2) headaches had at least one of the following three characteristics: pulsating quality, unilateral location, or aggravation by physical activity; and (3) during headaches, at least one of the following was present: nausea, photophobia, or phonophobia. The diagnoses were mutually exclusive, and a headache not satisfying the criteria for a migraine headache was classified as a nonmigrainous headache.

Our criteria for migraine headaches were a modified version of the migraine criteria of the International Headache Society.[5] The most notable modification was that severity of pain was not included among the pain characteristics. The questionnaire-based headache diagnoses were validated by an interview diagnosis reported in a separate article, including a discussion of the discrepancy between our migraine criteria and the International Headache Society criteria.[4] The positive and negative predictive values were 84 and 78% for migraine headaches and 68 and 76% for nonmigrainous headaches, respectively.[4]

The 1-year prevalence of migraine and nonmigrainous headaches was 12 and 26%, respectively.[6] Among those with nonmigrainous headaches, 80% had tension-type headaches according to our validation study.[4]

### *Statistical Analysis*

Differences between means were tested with an unpaired $t$ test. $p$ Values of less than 0.05 were considered statistically significant. We estimated prevalence odds ratios with 95% confidence intervals for the association between headache and hemochromatosis, and we evaluated potential confounding by age (5-year categories) and years of education ($<10$, 10–12, and $>12$) with unconditional logistic regression. Statistical analyses were performed with the Statistical Package for the Social Sciences, version 8.0 (SPSS, Chicago, IL).

The study was approved by the Regional Committee for Ethics in Medical Research and by the Norwegian Data Inspectorate.

## Results

High serum transferrin saturation in repeated tests was present in 496 subjects (240 men and 256 women) who responded to the headache questionnaire. We found no relation between headache prevalence and the level of serum transferrin saturation, and headache prevalence was similar among individuals with elevated serum ferritin in comparison with those with normal values (data not shown). Of the 496 persons with elevated serum transferrin saturation in two different tests, phenotypic hemochromatosis was diagnosed in 227 individuals (153 men and 74 women). As for age, the group with phenotypic hemochromatosis (mean, 49.6 years; SD, 14.8) did not differ from the general population (mean, 49.1 years; SD, 16.9; $p = 0.64$).

Among the 74 women with phenotypic hemochromatosis, the prevalence of headache was 80% higher (odds ratios, 1.8; 95% confidence interval, 1.1–2.9) than in those without phenotypic hemochromatosis (Table). This was most evident among women more than 60 years of age (Fig). Analyzing the data according to headache subtype, we found increased prevalence both of migraine and nonmigrainous headaches, with statistical significance reached for the latter (see Table). Among men, there was no clear relation between headache and hemochromatosis.

*Table. Prevalence Odds Ratio[a] for Headache according to Phenotypic Hemochromatosis and Genotype Status*

| Variable | N | All Headache Types | | | Nonmigrainous Headache | | | Migraine | | |
|---|---|---|---|---|---|---|---|---|---|---|
| | | n | OR | (95% CI) | n | OR | (95% CI) | n | OR | (95% CI) |
| Women | | | | | | | | | | |
| Phenotypic hemochromatosis | | | | | | | | | | |
| No | 27,380 | 12,792 | 1.0 | Reference | 8,372 | 1.0 | Reference | 4,420 | 1.0 | Reference |
| Yes | 74 | 44 | 1.8 | (1.1–2.9) | 30 | 1.8 | (1.1–3.1) | 14 | 1.7 | (0.9–3.2) |
| Genotype status | | | | | | | | | | |
| General population[b] | 27,380 | 12,792 | 1.0 | Reference | 8,372 | 1.0 | Reference | 4,420 | 1.0 | Reference |
| C282Y/C282Y | 102 | 62 | 1.8 | (1.2–2.8) | 45 | 2.0 | (1.3–3.1) | 17 | 1.4 | (0.8–2.6) |
| All other genotypes[c] | 138 | 67 | 0.9 | (0.7–1.3) | 47 | 1.0 | (0.7–1.5) | 20 | 0.8 | (0.5–1.4) |
| Men | | | | | | | | | | |
| Phenotypic hemochromatosis | | | | | | | | | | |
| No | 23,398 | 6,809 | 1.0 | Reference | 5,088 | 1.0 | Reference | 1,721 | 1.0 | Reference |
| Yes | 153 | 45 | 1.0 | (0.7–1.4) | 34 | 1.0 | (0.7–1.5) | 11 | 0.9 | (0.5–1.7) |
| Genotype status | | | | | | | | | | |
| General population[b] | 23,398 | 6,809 | 1.0 | Reference | 5,088 | 1.0 | Reference | 1,721 | 1.0 | Reference |
| C282Y/C282Y | 146 | 41 | 0.9 | (0.6–1.4) | 29 | 0.9 | (0.6–1.4) | 12 | 1.1 | (0.6–2.0) |
| All other genotypes[c] | 73 | 22 | 1.1 | (0.7–1.9) | 18 | 1.2 | (0.7–2.1) | 4 | 0.8 | (0.3–2.3) |

[a]Adjusted for age and education level.
[b]Not genotyped (normal serum transferrin saturation).
[c]Including C282Y/H63D, C282Y/W, H63D/H63D, H63D/W, and W/W (W = wild type).

CI = confidence interval.

Of the 496 participants with high serum transferrin saturation in two tests, 248 persons (146 men and 102 women) were homozygous for the C282Y mutation. The mean age of the latter group (mean, 49.4 years; SD, 15.4) was similar to that of the general population (mean, 49.1 years; SD, 16.9; $p = 0.76$). Again, the prevalence of headache in general and of nonmigrainous headaches was nearly twice as high among women homozygous for the C282Y mutation in comparison with the general population (see Table). The strongest association with headache was found among the 64 women with the C282Y/C282Y mutations and phenotypic hemochromatosis (odds ratios, 2.3; 95% confidence interval, 1.3–3.8).

Among men, no such relation was found. No increased prevalence of headache was found in those with other genotypes (see Table).

*Fig. One-year prevalence of headache with 95% confidence intervals in women with phenotypic hemochromomatosis (n = 74) and in the general female population (n = 27,380) by age (*p = 0.01). The chosen age categories divided the group of women with hemochromatosis into three equally large samples.*

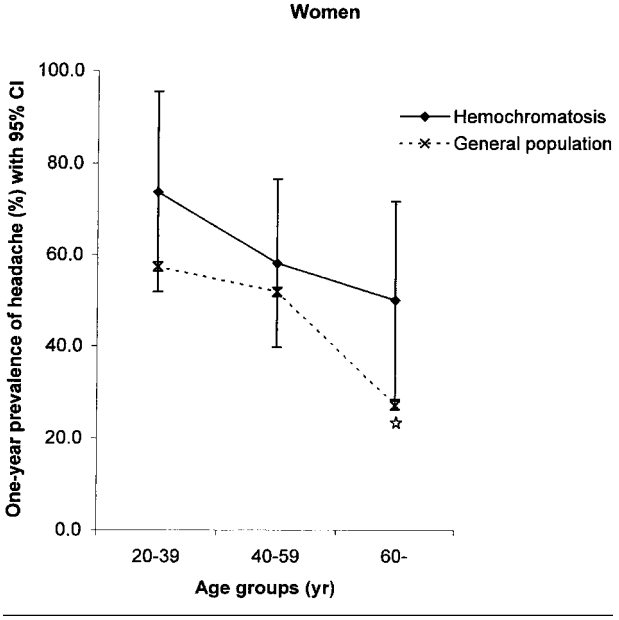


## Discussion

To the best of our knowledge, this is the first study evaluating the association between headache and hemochromatosis. The main finding was that women with previously undiagnosed and untreated phenotypic hemochromatosis and/or the C282Y/C282Y genotype had an 80% increased prevalence of headache.

The main strength of our study is the large unselected population sample, which includes the majority of the adults living in Nord-Trøndelag County. Because neither headache nor hemochromatosis screening was the primary objective of the study, interest-related bias appears unlikely. Furthermore, the participants were not aware of the diagnosis of hemochromatosis at the time they responded to the headache questions. Therefore, anxiety for such a disorder did not influence the participants' responses to the headache questions.

If bias can be excluded, the association between hemochromatosis and headache may be a causal one. One possible explanation of our findings may be that iron overload alters neuronal excitability and thereby lowers the threshold for triggering headache. It may be relevant that animal and human studies suggest that iron overload may be involved in the pathophysiology of epilepsy.[7,8] Also, in rats preloaded with iron, there has been observed an increased production of nitric oxide,[9] which is able to induce headaches.[10]

Welch and colleagues reported elevated iron levels in the periaqueductal gray matter of patients with migraines and chronic daily headaches.[11] Because iron levels in their study increased with the duration of illness, they suggested that iron accumulation in the headache patients could be caused by repeated headache attacks over time or, alternatively, could be involved as a causal headache factor.[11]

There was also an association between the C282Y/C282Y genotype and headache among women, although it was most evident for those who also had phenotypic hemochromatosis. It is possible that a high prevalence of headache may partly depend on this mutation rather than on the iron overload because we did not find any relation between headache and elevated transferrin saturation or elevated ferritin per se.

Why hemochromatosis was associated with headache only among women is unclear. This gender-specific finding is not an effect of a difference in statistical power, as hemochromatosis predominates among men. We may speculate that our finding reflects an interaction between female sex hormones and the C282Y/C282Y genotype isolated from or combined with iron overload.

Our findings should be followed by further investigations of headache complaints among female patients with hemochromatosis, and studies with high-resolution magnetic resonance techniques measuring the nonheme iron in brain tissues may be of special interest.

This study was supported by a grant from GlaxoSmithKline (Norway) and a research grant from the Norwegian Research Council (121953/330, K.H.).

## Appendix

The Nord-Trøndelag Health Study is a collaboration of the HUNT Research Centre, Faculty of Medicine, Norwegian University of Science and Technology (Verdal); the National Institute of Public Health; the National Health Screening Service of Norway; and the Nord-Trøndelag County Council.

## References

1. Powell LW, Subramaniam VN, Yapp TR. Haemochromatosis in the new millennium. J Hepatol 2000;32(suppl 1):48–62.
2. Benkovic SA, Connor JR. Ferritin, transferrin, and iron in selected regions of the adult and aged rat brain. J Comp Neurol 1993;338:97–113.
3. Åsberg A, Hveem K, Thorstensen K, et al. Screening for hemochromatosis: high prevalence and low morbidity in an unselected population of 65,238 persons. Scand J Gastroenterol 2001;36:1108–1115.
4. Hagen K, Zwart JA, Vatten L, et al. Head-HUNT: validity and reliability of a headache questionnaire in a large population-based study in Norway. Cephalalgia 2000;20:244–251.
5. Headache Classification Committee of the International Headache Society. Classification and diagnostic criteria for headache disorders, cranial neuralgias, and facial pain. Cepahalalgia 1988; 8(suppl 7):19–28.
6. Hagen K, Zwart JA, Vatten L, et al. Prevalence of migraine and non-migrainous headache—head-HUNT, a large population-based study. Cephalalgia 2000;20:900–906.
7. Ikeda M. Iron overload without the C282Y mutation in patients with epilepsy. J Neurol Neurosurg Psychiatry 2001;70: 551–553.
8. Campbell KA, Bank B, Milgram NW. Epileptogenic effects of electrolytic lesions in the hippocampus: role of iron deposition. Exp Neurol 1984;86:506–514.
9. Hida AI, Kawabata T, Minamiyama Y, Okada S. Iron preloading enhances lipopolysaccharide (LPS)-induced nitric oxide (NO) and cytokine production in vivo [abstract]. Paper presented at: Bioiron 2001 World Congress on Iron Metabolism; August 18–23, 2001; Cairns, Australia.
10. Olesen J, Thomsen LL, Lassen LH, Olesen IJ. The nitric oxide hypothesis of migraine and other vascular headaches. Cephalalgia 1995;15:94–100.
11. Welch KMA, Nagesh V, Aurora SK, Gelman N. Periaqueductal gray matter dysfunction in migraine: cause or the burden of illness? Headache 2001;41:629–637.

# Thrombolysis Induces Cerebral Hemorrhage in a Mouse Model of Cerebral Amyloid Angiopathy

David T. Winkler, MD, PhD,[1] Luc Biedermann, MS,[1] Markus Tolnay, MD,[1] Peter R. Allegrini, PhD,[2] Matthias Staufenbiel, PhD,[3] Christoph Wiessner, PhD,[3] and Mathias Jucker, PhD[1]

**We studied the impact of cerebral amyloid angiopathy on tissue plasminogen activator-induced cerebral hemorrhages in APP23 transgenic mice. Results show that the intravenous administration of tissue plasminogen activator in APP23 mice leads to an increase in cerebral amyloid angiopathy-associated microhemorrhages and can provoke parenchymal and subarachnoidal hematomas. We conclude that cerebral amyloid angiopathy is a risk factor for cerebral hemorrhage caused by tissue plasminogen activator administration in mice and stress the need for more comprehensive studies of the relation between cerebral amyloid angiopathy and tissue plasminogen activator-induced cerebral hemorrhages in elderly and Alzheimer's disease patients.**

Ann Neurol 2002;51:790–793

The systemic administration of tissue plasminogen activator (tPA) has become a standard treatment for myocardial infarct and is widely used for the early treatment of ischemic cerebral stroke and pulmonary embolism.[1–3] The outcome of this thrombolytic therapy is shadowed by possible side effects of fatal intracerebral hemorrhages (ICH).[4] The risk of tPA-induced ICH ranges from 0.5 to 1% for the treatment of myocardial infarct and pulmonary embolism[5,6] and reaches 6% in cerebral stroke patients.[7]

Cerebral amyloid angiopathy (CAA) is mostly a sporadic cerebral vasculopathy that causes about 10% of all nontraumatic ICH in the elderly.[8] Because both CAA-induced ICH and tPA-induced ICH increase in frequency with aging, occur often at multiple sites, and share a predominantly lobar localization, an interrelationship among tPA, CAA, and ICH has been suggested.[4,9,10]

The lack of animal models and limited diagnostic options for CAA have precluded a thorough study of the role of CAA in tPA-induced hemorrhages. We have previously reported that transgenic APP23 mice reproduce the typical findings of human CAA, namely, cerebrovascular amyloidosis, smooth muscle cell loss, microhemorrhages, and, in old age, spontaneous cerebral hematomas.[11,12] In the present study, we investigate the consequences of tPA administration in this mouse model of CAA.

## Materials and Methods

### *Animals and Tissue Plasminogen Activator Treatment*

Male 23-month-old APP23 mice[11,12] were anesthetized, and either saline (n = 12), 1mg/kg tPA (n = 12), or 10mg/kg tPA (n = 12) (Alteplase, Actilyse, Boehringer Ingelheim, Germany) was administered by the tail vein. The low dose corresponds to the dose used in humans for thrombolysis. The high dose was chosen because the clot–lysis system in rodents has been reported to be less responsive to tPA than that of humans.[13] An additional group of nontransgenic littermate control mice (n = 12) was treated with 10mg/kg tPA. Ten percent of the dose was given within the 1st minute, and the rest was given over 30 minutes with a micropump. Five mice died within 10 days after treatment (saline, 1; low-dose tPA, 3; high-dose tPA, 1; nontransgenic controls, 2).

### *Histology and Immunohistochemistry*

Ten days after treatment, mice were sacrificed, and serial 25μm paraffin sections were cut throughout the brain. Cresyl violet, hematoxylin and eosin, Congo red staining, the Berlin blue method of Perls, and immunohistochemistry with polyclonal antibody NT12 to Aβ were performed according to previously published protocols.[11,12]

### *Quantification of Cerebral Amyloid Angiopathy and Hemorrhage*

CAA was quantified with a previously described rating system.[12] In brief, the CAA frequency was obtained from the total number of affected vessels in a systematically sampled set of every 20th Aβ-immunostained section. For estimation of CAA severity, Aβ-positive vessels were classified into three severity grades.[12] A CAA score was obtained by multiplication of the CAA frequency with the CAA severity. One mouse was eliminated from the analysis because its CAA score exceeded the group mean by more than four times the standard deviation of the group.

Cerebral hemorrhage is followed by a delayed appearance of hemosiderin-positive microglia cells 5 to 7 days after the bleeding.[14] For the quantification number, Berlin blue-stained clusters of hemosiderin were assessed on sets of every 10th systematically sampled section throughout the entire neocortex.[12] An additional set of every 10th section was

From the [1]Department of Neuropathology, Institute of Pathology, University Hospital Basel, Basel, Switzerland, and [2]Core Technologies Area and [3]Nervous System Research, Novartis Pharma AG, Basel, Switzerland.

Received Nov 28, 2001, and in revised form Feb 13, 2002. Accepted for publication Feb 13, 2002.

Published online May 21, 2002, in Wiley InterScience (www.interscience.wiley.com). DOI: 10.1002/ana.10210

Address correspondence to Dr Jucker, Institute of Pathology, University of Basel, Schönbeinstrasse 40, CH-4003 Basel, Switzerland. E-mail: mjucker@uhbs.ch

 

stained for hematoxylin and eosin and screened for remnants of acute intraparenchymal or subarachnoidal hematomas. All quantification was performed by two raters (D.T.W. and L.B.) with interobserver correlations of $r = 0.80$ to 0.93.

*Magnetic Resonance Imaging*

Cerebral magnetic resonance imaging scans of randomly chosen mice (saline, 5; high-dose tPA, 7; nontransgenic controls, 5) were performed 4 to 7 days after tPA administration. Magnetic resonance imaging scans were taken on a 4.7T DBX spectrometer (Bruker, Karlsruhe, Germany).[15] In brief, the mice were anesthetized and subjected to one imaging cycle, in which T2-weighted 1mm-thick coronal brain slices were scanned with a RARE sequence (repetition time, 3,000msec; effective echo time, 88msec; spatial resolution in plane, 86$\mu m^2$). The total measuring time was 2.3 minutes.

## Results

Cerebrovascular amyloid was a reliable finding in the neocortex of all APP23 mice (Fig 1A, B). Mean CAA scores ± standard error of the mean (SEM) were 107.3 ± 9.9, 98.2 ± 8.4, and 94.2 ± 12.5 for the saline-treated group, the low tPA dose, and the high tPA dose, respectively. This observation is in line with previous estimates of CAA in aged APP23 mice.[12] No amyloid deposits were found in the nontransgenic control mice (Fig 1C).

Spontaneous cerebral microhemorrhages indicated by hemosiderin-positive perivascular microglia were found in all mice with CAA (see Fig 1D–F). Strikingly, tPA-treated APP23 mice showed robust increases in the number of microhemorrhages in comparison with saline-treated mice (Fig 2A), although an analysis of variance failed to reach statistical significance [$F(2,27) = 1.82$, $p > 0.05$]. However, when the microhemorrhage frequency was expressed in relation to the CAA scores (number of microhemorrhages/CAA score; see Fig 2B), an analysis of variance showed a statistically significant effect of treatment [$F(2,27) = 3.36$, $p < 0.05$]. A Newman-Keuls post hoc group comparison showed 93 and 67% increases in hemorrhages per CAA score between saline and low-dose tPA ($p < 0.05$) and saline and high-dose tPA ($p > 0.05$) respectively. Similar statistical significance per treatment was obtained with a Kruskal-Wallis analysis ($p < 0.05$) followed by a Mann-Whitney $U$ test between saline and low-dose tPA ($p < 0.01$).

Large hematomas with the presence of erythrocytes in the parenchyma or subarachnoid space were found in 1 of 9 mice treated with the low dose of tPA and in 2 of 11 mice treated with the high dose of tPA. No such hematomas or fresh bleedings were found in the saline-treated APP23 mice (Fig 3). One such hematoma could be identified before sacrifice in vivo by a T2-weighted magnetic resonance imaging scan (see Fig 3A and B). Histologically, the hematomas were surrounded by

*Fig 1. Cerebral amyloid angiopathy (CAA) and microhemorrhages in tissue plasminogen activator (tPA)-treated APP23 and nontransgenic control mice. Aβ immunostaining shows similar degrees of cerebrovascular amyloid in saline-treated (A) and tPA-treated (B) 23-month-old APP23 mice. Amyloid deposition is mainly confined to the vessel wall but spreads occasionally into the parenchyma (arrows indicate CAA grade 2 vessels; see the Materials and Methods section and Winkler and colleagues[12]). (C) No Aβ immunoreactivity is seen in nontransgenic control mice. The iron stain of Perls was used to detect microhemorrhages. Nearly twice as many hemorrhages (asterisks) were detected in APP23 mice treated with 1mg/kg tPA (E) than in saline-treated APP23 mice (D). (F) No hemorrhages were found in tPA-treated nontransgenic control mice. Arrows indicate vessels. Scale bar = 100μm and applies to all panels.*

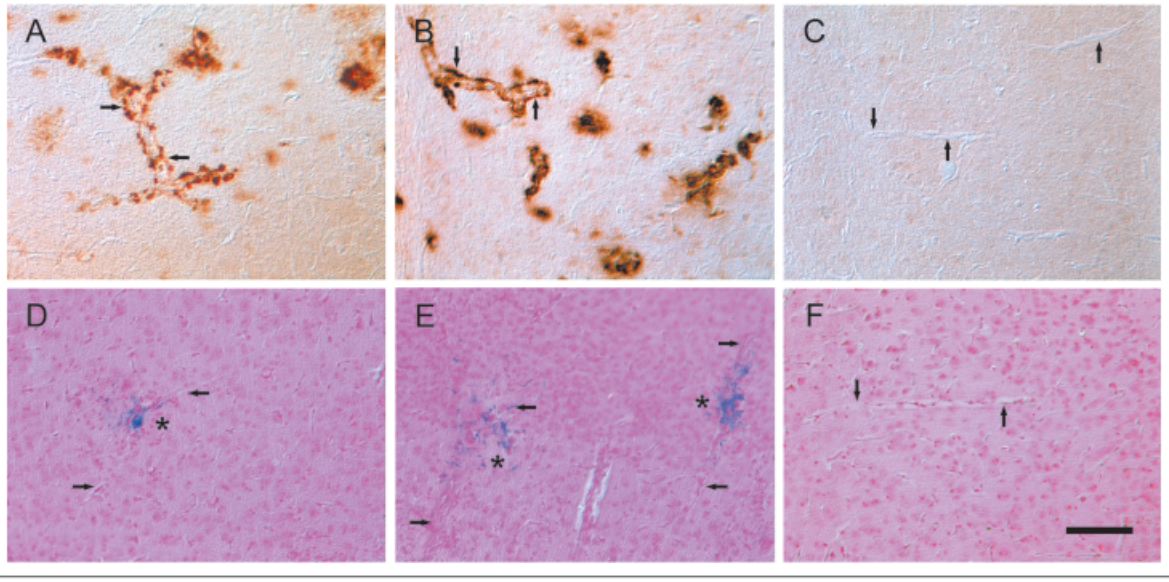

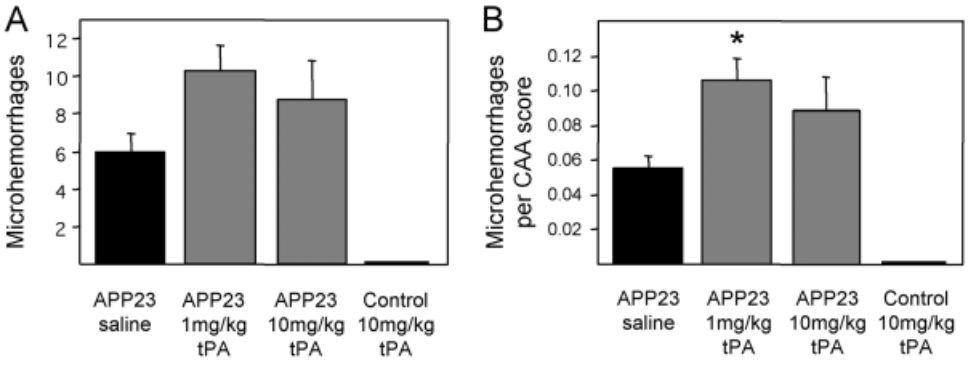


*Fig 2. Number of microhemorrhages in response to tissue plasminogen activator (tPA) treatment. (A) Frequency of microhemorrhages in 23-month-old APP23 mice treated with saline, 1mg/kg tPA, or 10mg/kg tPA. A considerable increase in the number of microhemorrhages (clusters of hemosiderin-positive perivascular microglia, as shown in Fig 1) was found in tPA-treated APP23 mice in comparison with saline-treated APP23 mice. Nontransgenic control mice treated with 10mg/kg tPA did not show any hemorrhages. (B) When the microhemorrhage frequency was expressed in relation to the cerebral amyloid angiopathy (CAA) score, 1mg/kg tPA treatment showed a nearly twofold increase in microhemorrhages* ($p < 0.05$).

hemosiderin-positive microglial cells (see Fig 3C and D). All 3 mice with hematomas showed high CAA scores (mean, 127.2; SEM, 26.2) and a high number of microhemorrhages (mean, 17.8; SEM, 2.1). No microhemorrhages or hematomas were detected in nontransgenic control mice treated with the high dose of tPA.

In most cases, bleedings could be easily allocated to amyloid-laden vessels. A positive correlation of CAA score and hemorrhage frequency was also found in all groups (saline, $r = 0.64$; low-dose tPA, $r = 0.66$; high-dose tPA, $r = 0.63$). Moreover, microhemorrhages were observed most frequently in the frontal cortex, matching CAA predominance in this region.

## Discussion

We have shown that the administration of tPA in a dose similar to that currently used in humans and with a protocol comparable to that currently used in humans results in an almost twofold increase in microhemorrhages in APP23 mice. This increase in hemorrhages in CAA-affected mice by tPA may be caused by lysis of microthrombi at sites of previous CAA-induced vascular injury.[16] In the context of this hypothesis, note that microthrombi are prone to tPA lysis only for a few days. Thereafter, fibrin is gradually lost from the thrombus and is replaced by the more stable collagen.[17] In addition to an increase in the hemosiderin-positive microhemorrhage number, we also found intraparenchymal and subarachnoidal hemorrhages in tPA-treated APP23 mice but not in nontransgenic control mice. This observation may be more similar to the human situation, in which tPA-induced cerebral hemorrhages tend to be more extensive than in the mouse. In humans, tPA fibrinolysis is usually combined with

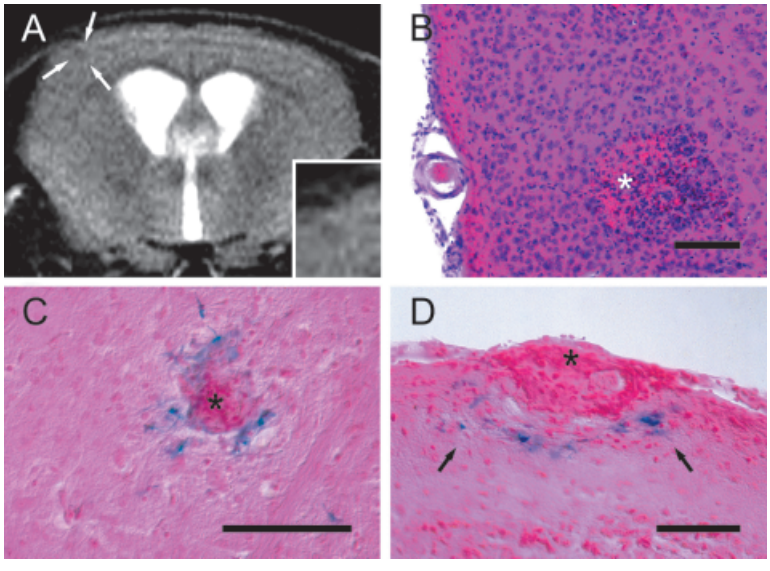


*Fig 3. Hematomas in tissue plasminogen activator-treated APP23 mice. (A) A T2-weighted magnetic resonance imaging scan showed a fresh cortical hematoma as a hypodense area (arrows) with a hyperdense perifocal zone (inset). (B) Subsequent hematoxylin and eosin staining confirmed the in vivo findings and showed a hematoma in this cortical region (asterisk). (C) A hematoma was also found in the striatum (asterisk). Note the hemosiderin-positive microglia in the periphery of the bleeding. (D) A subarachnoidal hemorrhage (asterisk) is shown with the cortical perifocal reactive zone (arrows). All scale bars = 100μm.*

heparin treatment that, in turn, may be a cause for the more severe hemorrhages observed in humans. Moreover, mice appear more resistant to cerebral hemorrhages because they do not develop spontaneous cerebral bleeding with aging, and tPA administration does not induce any microhemorrhages in wild-type mice.

In APP23 mice, tPA-induced microhemorrhages appear not to be dose-dependent. In contrast, a dose effect on tPA-induced hemorrhages has been reported in humans.[4] A similar dose effect, although based on small numbers, may occur in the mice with respect to larger hemorrhages. It is possible that for the lysis of small microthrombi, a low dose of tPA is sufficient, whereas for the removal of larger clots with subsequent large hematomas, a higher dose of tPA is needed.

We conclude that CAA is a significant risk factor for cerebral hemorrhages caused by tPA administration. This finding is of particular relevance for thrombolysis in elderly patients and in patients with Alzheimer's disease. Over 10% of people over 60 years of age and 80% of patients with Alzheimer's disease exhibit moderate CAA,[9] and tPA-induced hemorrhages are twice as frequent in elderly patients as compared with younger patients.[6] Therefore, the assessment of CAA appears crucial for successful tPA thrombolytic treatment. A diagnosis of probable CAA can now be obtained with gradient echo magnetic resonance imaging, which is used to identify small asymptomatic hemorrhages typically associated with CAA.[18] In addition, molecular risk factors of CAA and associated hemorrhagic stroke, such as apolipoprotein E, have been identified and may supplement CAA diagnosis.[19] Unfortunately, these diagnostic tools may be of limited use for emergency treatment when rapid tPA administration shortly after the vessel occlusion is requested.[2] Alternative therapeutic options for patients with a high risk of CAA are currently limited to mechanical interventions such as primary coronary angioplasty and the use of stents.[20] Therefore, the improvement of diagnostic tools for CAA and new therapeutic options for vessel-occluding diseases should be evaluated and are needed for patients with a high risk of CAA.

This work was supported by grants from the Swiss National Science Foundation (3100-056753.99, M.J., 3135-54877.98, D.T.W.) and the Thyssen Foundation (Cologne, Germany, Az. 2000-1077, M.J.).

We thank L. Walker (Ann Arbor, MI), S. M. Greenberg (Boston), and M. Pfeifer, D. Abramowski, Th. Mueggler, F. D'Amato, Th. Haffner, and W. Theilkäs (Basel) for their help and advice.

## References

1. Armstrong PW, Collen D. Fibrinolysis for acute myocardial infarction: current status and new horizons for pharmacological reperfusion, part 1. Circulation 2001;103:2862–2866.
2. Brott T, Bogousslavsky J. Treatment of acute ischemic stroke. N Engl J Med 2000;343:710–722.
3. Goldhaber SZ, Haire WD, Feldstein ML, et al. Alteplase versus heparin in acute pulmonary embolism: randomised trial assessing right-ventricular function and pulmonary perfusion. Lancet 1993;341:507–511.
4. Sloan MA, Price TR, Petito CK, et al. Clinical features and pathogenesis of intracerebral hemorrhage after rt-PA and heparin therapy for acute myocardial infarction: the thrombolysis in myocardial infarction (TIMI) II pilot and randomized clinical trial combined experience. Neurology 1995;45:649–658.
5. TIMI Study Group. Comparison of invasive and conservative strategies after treatment with intravenous tissue plasminogen activator in acute myocardial infarction. Results of the thrombolysis in myocardial infarction (TIMI) phase II trial. N Engl J Med 1989;320:618–627.
6. Gurwitz JH, Gore JM, Goldberg RJ, et al. Risk for intracranial hemorrhage after tissue plasminogen activator treatment for acute myocardial infarction. Participants in the National Registry of Myocardial Infarction 2. Ann Intern Med 1998;129:597–604.
7. Hacke W, Kaste M, Fieschi C, et al, for the Second European–Australasian Acute Stroke Study Investigators. Randomised double-blind placebo-controlled trial of thrombolytic therapy with intravenous alteplase in acute ischaemic stroke (ECASS II). Lancet 1998;352:1245–1251.
8. Itoh Y, Yamada M, Hayakawa M, et al. Cerebral amyloid angiopathy: a significant cause of cerebellar as well as lobar cerebral hemorrhage in the elderly. J Neurol Sci 1993;116:135–141.
9. Vinters HV. Cerebral amyloid angiopathy. A critical review. Stroke 1987;18:311–324.
10. Pendlebury WW, Iole ED, Tracy RP, Dill BA. Intracerebral hemorrhage related to cerebral amyloid angiopathy and t-PA treatment. Ann Neurol 1991;29:210–213.
11. Calhoun ME, Burgermeister P, Phinney AL, et al. Neuronal overexpression of mutant amyloid precursor protein results in prominent deposition of cerebrovascular amyloid. Proc Natl Acad Sci U S A 1999;96:14088–14093.
12. Winkler DT, Bondolfi L, Herzig MC, et al. Spontaneous hemorrhagic stroke in a mouse model of cerebral amyloid angiopathy. J Neurosci 2001;21:1619–1627.
13. Lijnen HR, van Hoef B, Beelen V, Collen D. Characterization of the murine plasma fibrinolytic system. Eur J Biochem 1994;224:863–871.
14. Koeppen AH, Dickson AC, McEvoy JA. The cellular reactions to experimental intracerebral hemorrhage. J Neurol Sci 1995;134(suppl):102–112.
15. Allegrini PR, Sauer D. Application of magnetic resonance imaging to the measurement of neurodegeneration in rat brain: MRI data correlate strongly with histology and enzymatic analysis. Magn Reson Imaging 1992;10:773–778.
16. Marder VJ, Sherry S. Thrombolytic therapy: current status. N Engl J Med 1988;318:1512–1520.
17. Jorgensen L, Rowsell HC, Hovig T, Mustard JF. Resolution and organization of platelet-rich mural thrombi in carotid arteries of swine. Am J Pathol 1967;51:681–719.
18. Knudsen KA, Rosand J, Karluk D, Greenberg SM. Clinical diagnosis of cerebral amyloid angiopathy: validation of the Boston criteria. Neurology 2001;56:537–539.
19. Nicoll JA, Burnett C, Love S, et al. High frequency of apolipoprotein E epsilon 2 allele in hemorrhage due to cerebral amyloid angiopathy. Ann Neurol 1997;41:716–721.
20. The Global Use of Strategies to Open Occluded Coronary Arteries in Acute Coronary Syndromes (GUSTO IIb) Angioplasty Substudy Investigators. A clinical trial comparing primary coronary angioplasty with tissue plasminogen activator for acute myocardial infarction. N Engl J Med 1997;336:1621–1628.